

## Diffusion in the Lorentz Gas

Carl P. Dettmann\*

School of Mathematics, University of Bristol, Bristol BS8 1TW, UK

(Received March 3, 2014; revised manuscript received April 8, 2014)

**Abstract** *The Lorentz gas, a point particle making mirror-like reflections from an extended collection of scatterers, has been a useful model of deterministic diffusion and related statistical properties for over a century. This survey summarises recent results, including periodic and aperiodic models, finite and infinite horizon, external fields, smooth or polygonal obstacles, and in the Boltzmann–Grad limit. New results are given for several moving particles and for obstacles with flat points. Finally, a variety of applications are presented.*

**PACS numbers:** 05.45.Ac, 05.60.Cd

**Key words:** Lorentz gas, Ehrenfest wind-tree model, conductivity, diffusion, Burnett coefficients

### 1 Introduction

The Lorentz gas was proposed by H.A. Lorentz in 1905<sup>[1]</sup> to model thermal and electrical conductivity of metals. The interactions between electrons were neglected, and the ions considered fixed, so the model consists of a single moving particle in an extended array of fixed scatterers. A Boltzmann-like approximation of uncorrelated collisions was made, so the implicit assumption was that the scatterers were of low density. Physically this makes sense (though ignoring electron-electron interactions and quantum effects) if the scatterers are reinterpreted as lattice defects rather than ions.

The subsequent century, especially the last decade, has seen a wealth of results on related models, with periodic, quasiperiodic and aperiodic scatterer arrangements, two, three and more dimensions, internal and external forces, and many other generalisations. Lorentz models have illuminated relevant fields, both mathematical (probability and dynamical systems) and in the physical sciences (foundations of statistical mechanics, molecular simulation, scattering and transport in periodic and random environments).

This review gives an overview of the latest developments, in particular since a previous survey by the same author;<sup>[2]</sup> see also Refs. [3–5]. There are also new calculations in Sec. 6 and (mostly old) open problems highlighted throughout. The order is logical rather than historical, starting with the widely investigated and relatively well understood periodic models and moving towards previously studied random models. The final section draws together some relevant applications. Corresponding quantum/wave systems are a huge and omitted field; see for example Refs. [6–8].

### 2 Preliminaries

#### 2.1 Microscopic Dynamics

A point particle with location  $\mathbf{x}(t) \in \mathbb{R}^d$  as a function of time  $t$ , moves freely except for reflections from an infinite collection of scatterers  $D_i \subset \mathbb{R}^d$ ; See Fig. 1. Free motion is at constant velocity of unit magnitude (without loss of generality), so

$$\frac{d\mathbf{x}}{dt} = \mathbf{v}, \quad |\mathbf{v}| = 1. \quad (1)$$

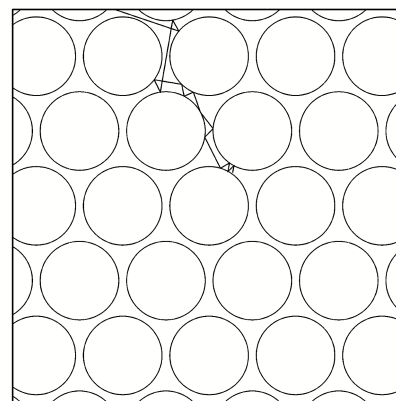


**Fig. 1** A triangular periodic Lorentz gas. This has finite horizon (see Subsec. 2.4), as there are no collision-free trajectories. Infinite horizon may be obtained with smaller scatterers or a square lattice.

This equation is solved together with that for the boundary to determine the time of next collision, a quadratic equation for the most common case of scatterers which are balls. After reaching a scatterer, a reflection takes place according to the usual rule that angle of reflection equal angle of incidence

$$\mathbf{v}_+ = \mathbf{v}_- - 2 \frac{\mathbf{v}_- \cdot \mathbf{n}}{\mathbf{n} \cdot \mathbf{n}} \mathbf{n}, \quad (2)$$

\*E-mail: Carl.Dettmann@bristol.ac.uk

where a centred dot denotes the usual scalar product and  $\mathbf{n}$  is a vector normal to the boundary. This formula does not require that  $\mathbf{n}$  be a unit vector, hence avoiding calculation of a square root.

Apart from the unbounded domain, the dynamics is exactly that of a mathematical billiard.<sup>[9–11]</sup> Basic properties of billiards which are useful in the Lorentz gas context are the existence of a uniform equilibrium measure, proportional to Lebesgue measure in position ( $\mathbb{R}^d$ ) and velocity ( $\mathbb{S}^{d-1}$ ) spaces, and invariant under the dynamics in the continuous time dynamics (billiard flow). For the billiard map (dynamics from one collision to the next) the corresponding measure is uniform on the boundary of the scatterer(s) and on the projection of velocity parallel to the boundary. With respect to this equilibrium measure there is an exact formula for the mean flight time between collisions

$$\langle \tau \rangle = \frac{|Q|S_{d-1}}{|\partial Q|V_{d-1}} = \frac{|Q|}{|\partial Q|} \frac{2\sqrt{\pi}\Gamma((d+1)/2)}{\Gamma(d/2)}, \quad (3)$$

where  $|Q|$  and  $|\partial Q|$  are the volume and surface of the billiard respectively, while  $V_d$  and  $S_{d-1}$  are the volume and surface of the  $d$ -dimensional unit ball respectively. Angle brackets denote expectation. For  $d = 2$  we find  $\pi|Q|/|\partial Q|$  and for  $d = 3$  we find  $4|Q|/|\partial Q|$ .

Another property derived from billiards is the symplectic structure of the dynamics, leading to a symmetric Lyapunov spectrum in the usual Hamiltonian fields (no field, electric and/or magnetic fields) and with Gaussian or Nosé–Hoover thermostats.<sup>[12–13]</sup> Also, the dynamics is time-reversible,<sup>[14]</sup> in that in all these cases except the magnetic field there is an involution  $\iota$  reversing the dynamics:  $\iota \circ \Phi^t \circ \iota = \Phi^{-t}$ . For the flow  $\iota$  is defined by reversal of velocity,  $\iota(\mathbf{x}, \mathbf{v}) = (\mathbf{x}, -\mathbf{v})$ , and for the map by the reflection law,  $\iota(\mathbf{x}, \mathbf{v}_-) = (\mathbf{x}, \mathbf{v}_+)$  from Eq. (2). Here,  $\Phi^t$  denotes the evolution forward by time  $t \in \mathbb{R}$  for the flow or collisions  $t \in \mathbb{Z}$  for the map.

Dynamical properties of billiards depend on the geometry of the boundary. We will assume the following unless stated explicitly:

**Definition 1** Dispersing billiard: All scatterers are disjoint, convex with strictly positive curvature and  $C^3$  smooth.

These requirements ensure that a parallel beam of initial conditions spreads out at each collision, leading to strongly chaotic properties (Subsec. 3.1). Various generalisations of the dynamics and dispersing condition are considered in later sections.

## 2.2 Diffusion

The main macroscopic property considered has been diffusion. For heat conduction see Ref. [15] and references therein, but note that the Lorentz gas collisions do not transfer energy, and so local thermal equilibrium is not generally satisfied.<sup>[16]</sup> Viscosity has also been considered.<sup>[17]</sup>

The displacement  $\Delta(t) = \mathbf{x}(t) - \mathbf{x}(0)$  is a deterministic function of the initial position and velocity. Considering a probability measure on the set of initial conditions and/or scatterer configurations, we can study the distribution of  $\Delta(t)$  including its moments as a function of  $t$ . Using  $i, j \in \{1, \dots, d\}$  as spatial indices, we can seek the following limiting properties, in roughly increasing order of strength:

**Current**

$$\mathbf{J} = \lim_{t \rightarrow \infty} \frac{1}{t} \langle \Delta \rangle. \quad (4)$$

If there is no external field, then the current is clearly zero due to time reversibility. If there is an external field, the following properties should be defined in terms of  $\Delta - \mathbf{J}t$ .

**Mean Square Displacement**

$$D_{ij} = \lim_{t \rightarrow \infty} \frac{1}{2t} \langle \Delta_i \Delta_j \rangle, \quad (5)$$

where  $D_{ij}$  is the diffusion matrix/tensor.

**Central Limit Theorem**

$$\frac{\Delta(t)}{\sqrt{t}} \Rightarrow \mathcal{N}(0, 2D_{ij}), \quad (6)$$

where  $\mathcal{N}$  is the multivariate normal distribution.

**Brownian Motion**

$$\frac{\Delta(st)}{\sqrt{t}} \Rightarrow W(s), \quad (7)$$

for  $s \in [0, 1]$ , where  $W$  is the standard  $d$ -dimensional Wiener process with covariance matrix  $2D_{ij}$ .

**Local Limit Theorem** Given an unbounded sequence of times  $t_n$  and scatterers with displacements  $\Delta_n/t_n \rightarrow \mathbf{x}$  and Voronoi cells (excluding the scatterers themselves) of volume  $V_n$ , the probability  $P_n$  of reaching the cell at time  $t_n$  has the expected limit:

$$\frac{t_n^{d/2} P_n}{V_n} \rightarrow \phi(\mathbf{x}), \quad (8)$$

where  $\phi$  is the density function of  $\mathcal{N}(0, 2D_{ij})$ .

Here,  $\Rightarrow$  denotes convergence in distribution as  $t \rightarrow \infty$ . The factors of two are required so that  $D_{ij}$  is the coefficient in the corresponding hydrodynamic equation

$$\frac{\partial}{\partial t} \rho = D_{ij} \frac{\partial}{\partial x_i} \frac{\partial}{\partial x_j} \rho, \quad (9)$$

where  $\rho(\mathbf{x}, t)$  is the density of particles. In cases with sufficient symmetry (e.g. triangular periodic or isotropic random Lorentz gases), the diffusion matrix is  $D_{ij} = D\delta_{ij}$  with  $D$  the diffusion coefficient. For more details see Sec. 2 of Ref. [18]. Note that anomalous versions of the above results hold in some situations; see Subsec. 4.2 for details.

## 2.3 Burnett Coefficients

It is sometimes useful to consider higher order diffusion processes. Generalising Ref. [19] slightly to allow for the non-isotropic case, we Fourier transform the density and expand in a formal power series, using subscripts for spatial indices. The derivation is given in two dimensions for clarity, but easily generalises to arbitrary dimension.

$$F(k_1, k_2, t) = \iint d\Delta_1 d\Delta_2 e^{-ik_1\Delta_1 - ik_2\Delta_2} \rho(\Delta_1, \Delta_2, t)$$

$$\begin{aligned}
&= \sum_{n_1=0}^{\infty} \sum_{n_2=0}^{\infty} \frac{(-i)^{n_1+n_2}}{n_1!n_2!} k_1^{n_1} k_2^{n_2} \langle \Delta_1^{n_1} \Delta_2^{n_2} \rangle \\
&= \exp \sum_{n_1=0}^{\infty} \sum_{n_2=0}^{\infty} \frac{(-i)^{n_1+n_2}}{n_1!n_2!} k_1^{n_1} k_2^{n_2} \langle \Delta_1^{n_1} \Delta_2^{n_2} \rangle_c, \quad (10)
\end{aligned}$$

by expanding the exponential in the first equation. The final equality defines the cumulants  $\langle \rangle_c$ , which have the important property that they are additive for independent random variables. We will use the notation  $M_{ab} = \langle \Delta_1^a \Delta_2^b \rangle$  for the moments and  $Q_{ab} = \langle \Delta_1^a \Delta_2^b \rangle_c$  for the cumulants. For example if odd moments are zero due to symmetry we have

$$\begin{aligned}
Q_{00} &= 0, \quad Q_{20} = M_{20}, \quad Q_{40} = M_{40} - 3M_{20}^2, \\
Q_{22} &= M_{22} - M_{20}M_{02}. \quad (11)
\end{aligned}$$

Differentiating Eq. (10), we find

$$F_t = F \sum_{n_1=0}^{\infty} \sum_{n_2=0}^{\infty} \frac{(-i)^{n_1+n_2}}{n_1!n_2!} k_1^{n_1} k_2^{n_2} \partial_t Q_{n_1 n_2}, \quad (12)$$

where the late time limit (if it exists) of the derivative is given by

$$\lim_{t \rightarrow \infty} \partial_t Q_{n_1 n_2} = \lim_{t \rightarrow \infty} \frac{1}{t} Q_{n_1 n_2}. \quad (13)$$

Thus we have

$$\begin{aligned}
\lim_{t \rightarrow \infty} \frac{F_t}{F} &= - \sum_{mn} D_{mn} k_m k_n \\
&+ \sum_{mnpq} B_{mnpq} k_m k_n k_p k_q + \dots, \quad (14)
\end{aligned}$$

with  $B$  the tensor form of the Burnett coefficient, as in Refs. [20–21]. Thus the Burnett coefficient can be interpreted as a fourth derivative term in Eq. (9).

Note that there are exactly the same number of independent  $B$  and  $Q$  coefficients for any dimension and level of symmetry; the even coefficients are related by

$$\begin{aligned}
D_{11} &= \lim_{t \rightarrow \infty} \frac{1}{2t} Q_{20}, \quad B_{1111} = \lim_{t \rightarrow \infty} \frac{1}{24t} Q_{40}, \\
B_{1122} &= \lim_{t \rightarrow \infty} \frac{1}{24t} Q_{22}. \quad (15)
\end{aligned}$$

This is a generalisation of Eq. (5); for the limit to exist, the term  $3M_{20}^2$  in Eq. (11) of order  $t^2$  needs to cancel an equivalent contribution from  $M_{40}$  to give a result of order  $t$ . Thus Burnett coefficients can be anomalous even when diffusion is normal.

The cumulants beyond second order are exactly zero for a normal distribution, and so quantify approach to it. The Burnett coefficients appear explicitly in corrections of local limit theorems in the case of independent random variables.<sup>[22]</sup>

## 2.4 Periodicity and Horizons

Periodic scatterer configurations are natural from both mathematical and physical perspectives. Mathematically, a periodic Lorentz gas is a  $\mathbb{Z}^d$  cover over a billiard in a torus, from which many useful properties may be derived;

in particular the equilibrium measure on the torus excluding the scatterer(s) is finite.

Physically, the Lorentz gas with circular/spherical scatterers of radius  $R$  is obtained by considering molecular dynamics of two particles of radius  $R/2$  with periodic boundary conditions in relative coordinates (that is, removing the uniform centre of mass motion).<sup>[2]</sup>

There is, however, an important issue to consider with periodic models. For the simplest case of a square lattice with non-overlapping circular scatterers, the particle can move freely parallel to a unit lattice vector without ever colliding with a scatterer; this property is called infinite horizon. For a triangular lattice with sufficiently large scatterers (as in Fig. 1) there is no such trajectory and the time between collisions is bounded; this is finite horizon. In aperiodic models (Sec. 7 below) a third possibility exists, where there is neither an infinite trajectory nor a bound on the collision time; this is locally finite horizon.

In three dimensions there may be cylinders and/or slabs of trajectories with no collisions, corresponding to “cylindrical” or “planar” infinite horizons; see Refs. [18, 23–24]. In general  $d \geq 2$  we consider the lattice  $\mathcal{L}$  of translations of the Lorentz gas. Following Refs. [18, 23] a free subspace is an inextendible linear subspace  $V \subset \mathbb{R}^d$  such that for a point  $\mathbf{x} \in \mathbb{R}^d$  the set  $\mathbf{x} + V$  does not intersect any scatterer (but may be tangent);  $V$  is a lattice subspace. The corresponding horizon is constructed by obtaining the maximal connected set  $B_H \subset \mathbf{x} + V^\perp$  containing  $\mathbf{x}$  that has  $V$  as a free subspace, where  $V^\perp$  is the linear space perpendicular to  $V$ . The horizon itself is the set

$$H = \{(\mathbf{x}, \mathbf{v}) : \mathbf{x} \in B_H + V, \mathbf{v} \in V \cap \mathbb{S}^{d-1}\}, \quad (16)$$

where the sphere  $\mathbb{S}^{d-1}$  imposes the restriction to unit speed. The dimension of the horizon  $d_H$  is the dimension of  $V$ , and satisfies  $1 \leq d_H \leq d - 1$ . A maximal horizon is a horizon of maximal dimension for a given Lorentz gas, a principal horizon is of dimension  $d - 1$ , and an incipient horizon is one in which  $B_H$  is zero  $d - d_H$  dimensional measure, for example a plane tangent to scatterers on both sides.

Let the free flight function  $F(t)$  be the probability (given initial conditions chosen according to the equilibrium measure) of not colliding before time  $t$ . Also, let  $F_H(t)$  be the probability of remaining in the spatial projection of the horizon  $B_H + V$  for time  $t$ . Then<sup>[18]</sup>

$$F_H(t) = \frac{S_{d_H-1} \int_{B_H} \int_{B_H} \Delta^{\text{vis}}(\mathbf{x}, \mathbf{y}) d\mathbf{x} d\mathbf{y}}{S_{d-1} \mathcal{V}_H^\perp (1 - \mathcal{P}) t^{d-d_H}}, \quad (17)$$

where  $\Delta^{\text{vis}}$  counts the number of ways  $\mathbf{x}$  and  $\mathbf{y}$  can be connected by a straight line entirely in  $B_H$ .  $\mathcal{V}_H^\perp$  is the volume of  $V^\perp / \mathcal{L}_V^\perp$  where  $\mathcal{L}_V^\perp$  is lattice obtained by the projection of  $\mathcal{L}$  on  $V^\perp$ . Finally  $\mathcal{P}$  is probability that an arbitrary point lies inside a scatterer.

Conjectured in Ref. [18] and proven in the preprint:<sup>[23]</sup>

$$F(t) \sim \sum_{H \in \mathbb{H}} F_H(t), \quad t \rightarrow \infty, \quad (18)$$

where  $\mathbb{H}$  is the set of maximal horizons if at least one is non-incipient. In the limit  $r \rightarrow 0$  the number of horizons diverges; a non-rigorous calculation using Mellin transforms yields for a  $d$ -dimensional cubic lattice<sup>[18]</sup>

$$\lim_{t \rightarrow \infty} tF(t) = \frac{\pi^{(d-1)/2}}{2^d d \Gamma((d+3)/2) \zeta(d) r^{d-1}} + O(r^{1/2-\delta}), \quad (19)$$

for  $\delta > 0$  subject to the Riemann Hypothesis, the major unsolved problem in number theory that asserts that the Riemann zeta function  $\zeta(s)$  has no zeros with real part greater than  $1/2$ .<sup>[25]</sup>

Also conjectured in Ref. [18] (except for the explicit exponent in the third case) and proven in Ref. [23]:

$$F(t) \asymp \begin{cases} t^{-2}, & 3 \leq d \leq 5, \\ t^{-2} \ln t, & d = 6, \\ t^{(2+d)/(2-d)}, & d > 6, \end{cases} \quad (20)$$

if there is at least one incipient (but no actual) principal horizon. The explicit exponent matches the numerical fits in Ref. [18] for  $d \leq 8$  beyond which the latter are not reliable. Note that the numerical simulations were carried out for cubic Lorentz gases with scatterers just touching, thus violating the dispersing condition.

**Open Problem 1** What is the form of  $F(t)$  if the maximal horizon is incipient but not principal?

In three or more dimensions, no periodic arrangement of spheres with a single sphere per unit cell has finite horizon. It is possible to create finite horizon configurations by having non-spherical scatterers, for example by considering a generic lattice and shrinking the Voronoi tessellation slightly to create strictly convex scatterers, or by a sufficiently large number of randomly placed spheres per unit cell.

**Open Problem 2** Find an explicit periodic arrangement of equal sized non-overlapping spheres with finite horizon in dimension  $d \geq 3$ .

### 3 Periodic with Finite Horizon

#### 3.1 Dynamical Properties

Dynamical properties of motion in a two-dimensional torus with strictly convex obstacles have been known since Sinai's 1970 paper<sup>[26]</sup> which showed that such systems exhibit the Kolmogorov property, which implies both ergodic properties (for example ergodicity and mixing) and hyperbolic properties (for example positive Lyapunov exponents for almost every initial condition). A modern detailed treatment of these questions for more general billiards may be found in Ref. [9].

Hyperbolicity holds for higher dimensional dispersing billiards (hence Lorentz gases), though in this case the structure of the singularities (due to tangential orbits) is much more involved.<sup>[27–28]</sup> These results extend automatically to the extended (Lorentz gas) case.

Ergodicity has been shown where the scatterers are algebraic varieties (such as spheres),<sup>[29]</sup> or when the

growth of singularities is less than exponential (and hence dominated by the exponential stretching associated with hyperbolicity)<sup>[30–31]</sup> however this condition known not to be always satisfied.<sup>[28]</sup> These difficulties were not appreciated before the turn of the millennium and so earlier results on higher dimensional Lorentz gases need to be treated with caution. The following assertion is however very likely true:

**Open Problem 3** Are all dispersing billiards on  $\mathbb{T}^d$  with  $d \geq 3$  and finite horizon ergodic?

References [30–31] prove a stronger ergodic property, that of exponential mixing of the billiard map, under this condition (sub-exponential complexity). This had been shown earlier for two-dimensional billiards by Young.<sup>[32]</sup> The rate of mixing for the flow is more difficult; the best results are stretched exponential in two dimensions,<sup>[33]</sup> with exponential only for billiards with a non-eclipsing condition (hence a finite number of scatterers in  $\mathbb{R}^2$ );<sup>[34]</sup> progress has been made on non-billiard models that are hyperbolic with singularities.<sup>[35]</sup>

A stronger result in another direction is the Bernoulli property for the map and flow, shown for all billiards in arbitrary dimension with non-zero Lyapunov exponents for both map and flow, and that satisfy the K-property.<sup>[36]</sup>

#### 3.2 Transport

Now we consider the dynamics in the extended space. In  $d \leq 2$ , the random walk is well known to be recurrent, with trajectories returning infinitely often arbitrarily close to their starting point. This holds also for the two-dimensional Lorentz gas, with the stronger property of ergodicity in the full space shown in Refs. [37–38]. Clearly this is not expected in higher dimensions.

The two-dimensional Lorentz gas has been shown to satisfy all the diffusive properties given in Subsec. 2.2: Bunimovich and Sinai showed convergence to Brownian motion in 1981,<sup>[39]</sup> the local limit theorem was proved by Szász and Varju in 2004<sup>[40]</sup> and the vector-valued almost sure invariance principle by Melbourne and Nicol in 2009.<sup>[41]</sup> In higher dimensions, the central limit theorem was shown in Ref. [30] under the condition of subexponential complexity.

**Open Problem 4** Are convergence to a Wiener process and local limit theorems satisfied for  $d \geq 3$ ?

Noting

$$\Delta_i = \int_0^t v_i(s) ds$$

we arrive at the expression<sup>[42]</sup>

$$\frac{1}{2} \langle \Delta_i \Delta_j \rangle = t \int_0^t \langle v_i(0) v_j(s) \rangle ds - \int_0^t s \langle v_i(0) v_j(s) \rangle ds, \quad (21)$$

which after division by  $t$  and taking the limit gives the continuous time version of the Green–Kubo formula for the diffusion coefficient  $D$ ; similar expressions apply to other transport coefficients such as viscosity and heat

conductivity.<sup>[43]</sup> The equivalent expression for the fourth order Burnett coefficients involves four-time correlation functions.<sup>[20]</sup>

Convergence of the integral follows from sufficiently rapid decay of the velocity autocorrelation function; this was shown to be (at least) a stretched exponential in Ref. [39]; similar multiple correlations were used in Refs. [21, 44] to show that Burnett coefficients of all orders also exist in the two-dimensional case.

There is no known closed form expression for the diffusion coefficient  $D$ , so there have been several analytical and numerical studies to approximate it. In the limit of small gaps between scatterers the time between moving from one gap to another is typically long and hence uncorrelated.<sup>[45]</sup> More sophisticated models extend this to take into account some correlations, for example Markov chains with finite memory.<sup>[46–48]</sup> There is also a study of three-dimensional Lorentz gases using this approach<sup>[49]</sup> including both finite and infinite horizon regimes (Sec. 4 below).

Alternative expressions for  $D$  exist in terms of periodic orbits of the torus dynamics (which are either periodic or translating in the full space). Considering only orbits up to a maximum length yields an approximation to the diffusion coefficient; see Refs. [50–52]. A rigorous basis of periodic orbit expansions is provided in Ref. [53].

There are simpler models of deterministic diffusion, for example one dimensional piecewise linear maps. Some models have a dense set of parameter values at which there is a finite Markov partition and hence the diffusion coefficient may be determined exactly using Markov chains or periodic orbits.<sup>[54–57]</sup> The diffusion coefficient is a fractal function of parameters (denoted  $\lambda$ ), for which the non-smoothness has been fairly well quantified,<sup>[58]</sup> being slightly less smooth than Lipschitz. An upper bound of the variation is

$$|D(\lambda) - D(\lambda')| < K|\lambda - \lambda'|(1 + \ln|\lambda - \lambda'|)^2, \quad (22)$$

while a lower bound includes a single power of the logarithm. The density dependence of the diffusion coefficient in the Lorentz gas is expected to be smoother (since the flow is continuous if the pre- and post- collisional states are considered connected); discussion and numerical results were presented in Ref. [46] and for a “flower” Lorentz gas in Ref. [59].

**Open Problem 5** How smooth is the diffusion coefficient of the Lorentz gas as a function of density?

### 3.3 External Fields

#### (i) Weak Field and Thermostat

The diffusion can also be calculated as the zero field limit of the non-equilibrium conductivity<sup>[60]</sup> (Eq. (27) below), a standard approach for transport coefficients in molecular simulation.<sup>[43]</sup> In this case an electric field is imposed, that provides a constant force on the particle

(assumed charged, though still not interacting with other moving particles). In order to prevent an unbounded growth of the particle’s energy, a thermostat force is also applied, as commonly used in molecular simulation.<sup>[12,43]</sup> The most commonly used thermostat in this context is the Gaussian isokinetic thermostat, for which the equation of motion is

$$\frac{d\mathbf{v}}{dt} = \mathbf{E} - \frac{\mathbf{E} \cdot \mathbf{v}}{\mathbf{v} \cdot \mathbf{v}}, \quad (23)$$

where  $\mathbf{E}$  is the constant electric field; the mass and charge are assumed equal to unity. This equation has the following properties:<sup>[12]</sup>

- The kinetic energy  $\mathbf{v} \cdot \mathbf{v}/2$  is conserved (hence the designation “isokinetic”) and so it is usually assumed that the velocity has unit magnitude.
- The involution  $\iota(\mathbf{x}, \mathbf{v}) = (\mathbf{x}, -\mathbf{v})$  reverses the motion (see Subsec. 2.1).
- The dynamics is conformally symplectic.<sup>[13,61]</sup> This means that in two dimensions there is a conformal transformation to a field-free billiard<sup>[13]</sup> and that in higher dimensions there is a symmetry of the Lyapunov spectrum, sometimes called the conjugate pairing rule.<sup>[13,62]</sup> Before the latter was shown, the three-dimensional Lorentz gas was used as a convenient system for numerical tests.<sup>[63]</sup>

If the electric field is to the right ( $\mathbf{E} = E\mathbf{e}_x$ ) and the direction of motion  $\mathbf{v} = (\cos\theta, \sin\theta)$  in the  $(x, y)$  plane (without loss of generality), the equation of motion reduces to  $d\theta/dt = -F \sin\theta$  with solution

$$\tan \frac{\theta}{2} = \tan \frac{\theta_0}{2} \exp \left[ -\frac{t - t_0}{E} \right], \quad (24)$$

$$x = x_0 - \frac{1}{E} \ln \frac{\sin \theta}{\sin \theta_0}, \quad (25)$$

$$y = y_0 - \frac{\theta - \theta_0}{E}. \quad (26)$$

Note that the motion in  $y$  (i.e. transverse to the field) is bounded by  $\pi/E$ . The equation determining the collision with a spherical scatterer is transcendental, however the shortest distance to a scatterer is a rigorous lower bound on the time, and leads to a quadratically convergent numerical algorithm.<sup>[63]</sup>

The two-dimensional finite horizon non-equilibrium Lorentz gas was considered in Ref. [64], where it was shown that for sufficiently small field the system remains ergodic, with a measure that is supported on the full phase space but singular (multifractal) with respect to the equilibrium measure. They give rigorous proofs of relations long stated in non-equilibrium physics, for example the existence of a well-defined current  $\mathbf{J}(\mathbf{E})$  (the average velocity) related in the limit of small field to the diffusion coefficient (or in low symmetry cases, tensor) by the Einstein relation

$$\mathbf{J} = D\mathbf{E} + o(\mathbf{E}). \quad (27)$$

Also, the diffusion tensor is continuous at zero field, the sum of the Lyapunov exponents comes to

$$\lambda_+ + \lambda_- = -\mathbf{J} \cdot \mathbf{E}, \quad (28)$$

and the information dimension of the flow (Hausdorff dimension of the measure) is given by the application of the Kaplan–Yorke–Young formula,<sup>[65]</sup>

$$D_1 = 2 + \frac{\lambda_+}{|\lambda_-|} = 3 - \frac{\mathbf{J} \cdot \mathbf{E}}{\lambda_0} + o(\mathbf{E}^2), \quad (29)$$

where  $\lambda_0$  is the magnitude of either of the Lyapunov exponents at zero field. Recently, Ref. [66] shows that the spatial projection of the ergodic measure is absolutely continuous. These authors also used a Gaussian thermostat as a coupling mechanism in a multiparticle driven Lorentz gas.<sup>[67]</sup>

### (ii) *Other Weak Fields and Thermostats*

Reference [64] incorporates a more general case of a weak magnetic field; since the magnetic force is perpendicular to the velocity it does not affect the strength of the thermostat and hence the sum of the Lyapunov exponents. It does however break the time reversibility (see Sec. 2.1). These results have been generalised in a number of papers: Ref. [68] considers more general small forces, Refs. [69–70] consider perturbed reflection functions, and Ref. [71] considers more general models with small forces and collision perturbations satisfying a conserved energy with compact phase space (cf the Galton board below) and time reversibility. Reference [71] extends the perturbations to include shifted, rotated or deformed scatterers and/or shifts at collision. The results are similar, including generalisations of the Einstein formulas. There are also studies of electric and magnetic fields in random Lorentz gases, discussed below in Subsec. 7.4.

From the point of view of molecular dynamics, there are a number of other thermostats in use.<sup>[12,72]</sup> The Nosé–Hoover thermostat retains reversibility and symplectic properties, while adding a degree of freedom. Its application to the Lorentz gas was considered numerically in Ref. [73], leading again to multifractal attractors but somewhat different bifurcation structure at strong field. It was used as an example of fluctuation theorems in Refs. [74–75].

Other deterministic thermostatting approaches have been less common, lacking time-reversibility and Hamiltonian structure. The constant friction thermostat was considered in Ref. [76] as an example of a non-reversible model, again studying the multifractal attractors. Note that there are some subtleties to the definition of reversibility; it turns out that if the attracting fixed point is excluded, the constant friction harmonic oscillator dynamics  $(\dot{x}, \dot{v}) = (v, -x - \alpha v)$  may be reversed by the involution

$$\iota(x, v) = \frac{(x, -v - \alpha x)}{x^2 + (v + \alpha x/2)^2 / (1 - \alpha^2/4)}. \quad (30)$$

A reversible thermostat-like model was considered numerically in Ref. [77]. There, the motion was as in a

billiard except that when the particle leaves via a boundary, returning on the opposite side, a dilation was applied, giving an effective field. A steady current was observed, linear in the field strength for weak field. Fluctuation relations studied. Infinite horizon and polygonal variants were also considered (see later sections).

### (iii) *Strong Field and Thermostat*

Some statements can be made about the Gaussian thermostat for strong fields. In the two-dimensional case, the conformal transformation to a field-free billiard<sup>[13]</sup> guarantees ergodicity as long as the appropriate conditions are satisfied:  $|\mathbf{E}| < \kappa_{\min}$  where  $\kappa_{\min}$  is the minimum curvature of the scatterers ensures that the dispersing condition is met; the finite horizon condition on the transformed billiard also needs to be checked. Smoothness of the current as a function of field is also of long interest: **Open Problem 6** How smooth is the current as a function of field?

A plot of this function is given in Ref. [2]. For larger fields, ergodicity appears to be broken by one of two mechanisms, elliptic stability of a periodic orbit (breaking of the above condition) or crisis where an attractor and its time reverse at high fields merge as the field is reduced.<sup>[78–79]</sup> At high fields the attractor(s) may be fractal or stable periodic orbits.

### (iv) *The Galton Board*

The Galton board or quincunx, predates the Lorentz gas,<sup>[80]</sup> consisting of a periodic Lorentz gas with a constant field but no thermostat. It was proposed and is still used as a mechanical demonstration of the binomial distribution, in which the particle falls under the action of a gravitational field through a triangular lattice of obstacles, moving left or right with approximately equal and independent probabilities (due to the rapid decay of correlations). The mechanical models have various sources of friction, but it is clear that the idealised model has unbounded kinetic energy as the particle continues to fall.

This model was studied rigorously in Ref. [81] with some unexpected results: The position of the particle grows on average as  $t^{2/3}$ , so there is no linear drift. From conservation of energy this means the speed grows as  $t^{1/3}$  (these had been obtained previously in the physics literature<sup>[82–83]</sup>). However the motion is also recurrent: The particle returns infinitely many times to the vicinity of its starting point. Note that the region containing the slowest motion is not a small perturbation of the field-free Lorentz gas, and so needs to be excluded (for example it is possible to have an elliptic periodic orbit bouncing between two scatterers).

## 4 Periodic with Infinite Horizon

### 4.1 *Dynamical Properties*

The local dynamics of Lorentz gases with infinite horizon, such as a cubic lattice of spheres for  $d \geq 2$  is some-

what more involved due to orbits which are tangent to infinitely many scatterers. In the vicinity of such orbits are an infinite number of singularities corresponding to orbits tangent to more and more remote scatterers. However, the billiard map in two dimensions still satisfies exponential decay of correlations.<sup>[84]</sup>

For the flow, results are given in Ref. [85]: The decay of correlations is known to be  $O(1/t^{1-\epsilon})$  for general infinite horizon Lorentz gases and explicitly  $C/t$  for the standard example of a square lattice of disks. The space of functions considered does not include position or velocity, however. Extension to the  $C/t$  result for arbitrary two-dimensional Lorentz gases is claimed in a later preprint.<sup>[86]</sup>

The situation for decay of correlations for infinite horizon Lorentz gases in higher dimensions, even under reasonable assumptions, appears to be open; see for example Ref. [31]. For the map it is likely exponential, while for the flow it likely has the same asymptotic form as  $F(t)$ , see Ref. [18].

## 4.2 Transport

The two-dimensional case is now relatively well understood, following a number of approximate/numerical<sup>[42,87–88]</sup> and rigorous<sup>[42,89–90]</sup> studies. Recurrence and ergodicity in the full space continue to hold, despite anomalous scaling. Detailed estimates for the recurrence properties (for example first return time distribution) for a related random walk model may be found in Ref. [91]. The current is typically well defined if an external field is not parallel to a horizon.<sup>[90]</sup> The long flights lead to the other equations of Subsec. 2.2 modified as follows:

### Mean Square Displacement

$$\mathcal{D}_{ij} = \lim_{t \rightarrow \infty} \frac{1}{2t \ln t} \langle \Delta_i \Delta_j \rangle, \quad (31)$$

where now  $\mathcal{D}_{ij}$  is a superdiffusion matrix/tensor.

### Central Limit Theorem

$$\frac{\Delta(t)}{\sqrt{t \ln t}} \Rightarrow \mathcal{N}(0, \mathcal{D}_{ij}), \quad (32)$$

where  $\mathcal{N}$  is the multivariate normal distribution.

### Brownian Motion

$$\frac{\Delta(st)}{\sqrt{t \ln t}} \Rightarrow W(s), \quad (33)$$

for  $s \in [0, 1]$ , where  $W$  is the standard  $d$ -dimensional Wiener process with covariance matrix  $\mathcal{D}_{ij}$ .

### Local Limit Theorem

Given an unbounded sequence of times  $t_n$  and scatterers with displacements  $\Delta_n/t_n \rightarrow \mathbf{x}$  and Voronoi cells (excluding the scatterers themselves) of volume  $V_n$ , the probability  $P_n$  of reaching the cell at time  $t_n$  has the expected limit:

$$\frac{(t_n \ln t_n)^{d/2} P_n}{V_n} \rightarrow \phi(\mathbf{x}), \quad (34)$$

where  $\phi$  is the density function of  $\mathcal{N}(0, \mathcal{D}_{ij})$ .

The inconsistency with regard to factors of two compared with the normal diffusion case was not noted until 2011; see Refs. [18, 92], where a history and heuristic argument may be found. Briefly, convergence in distribution does not imply convergence of the moments, and in this case as  $t \rightarrow \infty$  the tails of the distribution decay in time while increasing in extent so that contribution to the mean square displacement from the tails does not decay, and in fact remains roughly equal to that from the limiting normal distribution. Recent results on convergence of moments in fairly general dynamical systems (not including the infinite horizon Lorentz gas) may be found in Ref. [93].

Reference [92] specifically considers anomalous convergence of moments, but in the context of billiards with cusps, that is, with the time to collision arbitrarily small. In this case the decay of correlations are algebraic for the map, but rapid for the flow.<sup>[94]</sup> As with the infinite horizon Lorentz gas (and also the stadium billiard<sup>[95]</sup> a nonstandard (logarithmic) central limit theorem applies.<sup>[96]</sup>

In contrast to the normal diffusion case (for example finite horizon), the superdiffusion coefficient  $\mathcal{D}$  can be expressed exactly in terms of the geometry of the horizons (ie set of infinite orbits). Expressions are given for two dimensions in Refs. [40, 42, 90]. In general we have (cf Subsec. 2.4):

$$\mathcal{D}_{ij} = \frac{1}{1 - \mathcal{P}} \frac{V_{d-1}}{S_{d-1}} \sum_{H \in \mathbb{H}} \frac{w_H^2 (\delta_{ij} - n_i(H) n_j(H))}{\mathcal{V}_H^\perp}, \quad (35)$$

if there is at least one non-incipient principal horizon, and for  $d \geq 3$  subject to a conjecture that correlations decay more rapidly than  $C/t$  restricted to trajectories with at least one collision.<sup>[18]</sup> Here,  $V_{d-1}$  is the volume of a  $(d-1)$ -dimensional ball,  $w_H$  is the width of the horizon (that is, one dimensional volume of  $B_H$ ) and  $\mathbf{n}(H)$  is a unit vector parallel to  $B_H$ .

If the maximal horizon is not principal, we expect that correlations decay as  $1/t^{d-d_H}$ , and thus from Eq. (21) that the normal diffusion coefficient exists (at least in terms of mean square displacement). As with finite horizon this is not accessible in closed form, but may be approximated using correlated random walks.<sup>[49]</sup> As discussed in Ref. [90], if the horizon directions do not span the full space, diffusion is anomalous in directions spanned by the horizons but normal in other directions.

## 4.3 External Fields

Reference [90] also considers superdiffusion with a Gaussian thermostat, finding

$$\mathbf{J} = \frac{1}{2} \mathcal{D} \mathbf{E} \ln |\mathbf{E}| + O(\mathbf{E}), \quad (36)$$

as long as the field is not parallel to a corridor (and the constant in the error term may depend on the direction of  $\mathbf{E}$ ). The special case with corridors in only a single

direction is also covered. When the field is parallel to a corridor, motion in this direction is an absorbing state, so all but a set of zero measure of initial conditions achieve this.

For the Galton board with infinite horizon the scaling  $v \sim (t \ln t)^{1/3}$  was conjectured in Ref. [83].

The thermostat-type model of Ref. [77] (see Subsec. 3.3(ii)) was also considered in an infinite horizon regime. As above, the conductivity (current divided by field) was numerically observed to be logarithmic in the field.

## 5 Alternative Limits

Two limits that are required for a study of diffusion are  $t \rightarrow \infty$  and  $L \rightarrow \infty$  where  $L$  is a length scale. We have seen that for normal diffusion (for example finite horizon Lorentz gases) these may be taken together, with  $L = c\sqrt{t}$  to give an appropriate limit law. Similarly  $L = c\sqrt{t \ln t}$  for the kind of superdiffusion found with principal infinite horizons. Other limits are also useful to consider, also involving the scatterer radius  $r$ .

### 5.1 Escape from Finite Domains

The “escape rate formalism” originated with Gaspard and Nicolis;<sup>[97]</sup> see also Refs. [20, 98]. Here we consider a finite horizon Lorentz gas on a finite domain, say a square of side length  $L$  (infinite domains such as a strip have also been considered). Scatterers from a periodic lattice are present inside the square, but the region outside is empty (or else the particle is absorbed when it reaches the boundary). Uniformly distributed initial conditions leak out, with a survival probability  $P(t)$  decaying exponentially in time  $t$  due to the strongly chaotic dynamics. The escape rate is

$$\gamma = - \lim_{t \rightarrow \infty} \frac{1}{t} \ln P(t). \quad (37)$$

Results relating escape rates with Lyapunov exponents and entropy in a general setting and for the two-dimensional finite horizon Lorentz gas are proven in Ref. [99]. This includes the “escape rate formula”, long known in simpler contexts:<sup>[100–101]</sup>

$$\gamma = \lambda - h_{\text{KS}}, \quad (38)$$

where the Lyapunov exponent and entropy refer to the natural invariant measure on the non-escaping set. Again, there is a Young formula for dimension<sup>[20, 65]</sup> corresponding to Eq. (29), although this does not appear to have been discussed for the Lorentz gas in the recent rigorous literature

$$D_I = 1 + \frac{2h_{\text{KS}}}{\lambda} = 3 - \frac{2\gamma}{\lambda}. \quad (39)$$

We have taken the  $t \rightarrow \infty$  limit at fixed  $L$ . Now, for large  $L$  we can compare with the hydrodynamic limit, Eq. (9) with the appropriate absorbing (i.e. Dirichlet)

boundary conditions. For example, in the case of the square  $[0, L]^2$  and isotropic diffusion matrix  $D_{ij} = D\delta_{ij}$ , the density

$$\rho = e^{-\gamma t} \sin \frac{\pi x}{L} \sin \frac{\pi y}{L} \quad (40)$$

is the lowest mode of Eq. (9) if

$$\gamma = \frac{2D\pi^2}{L^2}. \quad (41)$$

Thus we can express the diffusion coefficient in terms of the escape rate and take the limit  $L \rightarrow \infty$ . Similar approaches can be made for other transport coefficients such as viscosity.<sup>[102]</sup> While not a practical method of computing transport coefficients, it does not modify the equations of motion (unlike the Gaussian thermostat in Subsec. 3.3(i) above), and so is easier to justify from a physical point of view.

In the infinite horizon case, little is known, though there is recent work where the lattice is infinite and holes are located in the reduced space.<sup>[103]</sup>

**Open Problem 7** Quantify the time-dependence of the survival probability and size-dependence of the escape rate for an open infinite horizon Lorentz gas.

A boundary between two finite Lorentz gases with different parameters was recently considered in Ref. [104]. This work demonstrated the need for a careful treatment of boundary conditions when considering hydrodynamic limits, namely that the diffusion equation is not a complete description of the macroscopic system.

### 5.2 The Boltzmann–Grad Limit

Here, the scatterer radius is taken to zero, but the spacing is also reduced so that the mean free path remains fixed, as is useful in kinetic theory of low density gases, for example the Boltzmann equation. The distribution of path lengths has explicit formulae available in two dimensions.<sup>[105–106]</sup> It turns out that the linear Boltzmann equation used by Lorentz for the random model (Subsec. 7.4 below) needs to be generalised, since for periodic models the limiting process has a kernel that depends not only on the initial and final velocities at a single collision, but also the flight time and velocity following a subsequent collision.<sup>[107–109]</sup> The resulting linear operator does not satisfy the semigroup property, despite being the zero radius limit of operators that do.

Marklof and Strömbergsson extended this to arbitrary dimension; technical proofs are found in Refs. [110–112]. The tail of the (closely related) free flight function in all dimensions agrees with the leading term of Eq. (19) despite the differing manner in which the limit is taken.<sup>[18]</sup> Marklof and Tóth have recently proved a central limit theorem, also in arbitrary dimension.<sup>[113]</sup> Their approach, which uses dynamics in the space of lattices, has also led

to interesting results in other fields, such as the distribution of Frobenius numbers.<sup>[114]</sup> Readable reviews of the work in this section are given in Refs. [115–116].

## 6 Semi- and Non- Dispersing Models

### 6.1 Molecular Dynamics

#### (i) General Discussion

Much of the physical motivation for the periodic Lorentz gas is for understanding molecular dynamics, models of many atoms moving under Newton's laws, often using periodic boundary conditions.<sup>[2,43]</sup> These models shed light on theoretical issues, such as the foundations of statistical mechanics, and the numerical simulations allow computation of how the bulk properties of materials depend on the microscopic force laws and parameters such as energy and volume per particle. The use of periodic boundary conditions avoids boundary effects, so bulk properties can be estimated with fewer particles.

The Lorentz gas as we have discussed so far is equivalent to a two particle system after transformation into (trivial) centre of mass motion and the relative motion of the particles. With three or more particles, there is still equivalence with a high dimensional periodic billiard, however the dispersing condition needs to be relaxed. There are various definitions of “semidispersing” billiards in the literature; here we want to allow cylindrical curvature, that is, positive curvature at all points, but not in all directions. Physically, when two particles collide, the outcome is indifferent to the location and motion of the remaining particle(s).

The system of many hard particles has been a major motivation and stimulus for the development of ergodic theory.<sup>[117]</sup> Hyperbolicity is now known for all hard ball systems.<sup>[118]</sup> Ergodicity is known when  $N = 2$  (as above),<sup>[119]</sup>  $N = 3$ ,<sup>[120]</sup>  $N = 4$  for  $d \geq 3$ <sup>[121]</sup> and general  $N \leq d$ ,<sup>[122–123]</sup> see also Ref. [29]. More recently ergodicity has been shown for almost all parameters (masses and a single radius),<sup>[124]</sup> and conditional on the Chernov–Sinai ansatz, the statement that almost every singular orbit is hyperbolic.<sup>[125]</sup> Finally, there is a complete proof in full generality.<sup>[126]</sup>

While an impressive result, this does not spell the end of the subject.<sup>[127]</sup>

**Open Problem 8** Is the system of hard balls in a hard box ergodic?

#### (ii) Infinite Horizon Effects

The periodic boundary conditions usually lead to infinite horizon effects, that is, there are trajectories in which one or more (usually all) of the particles never collide. The following is a previously unpublished study, mostly restricted to  $N = 3$  on a unit 2-torus and with all masses and radii equal and zero total momentum.

First note that if there are no collisions, the relative displacements of pairs of particles are tracing out a lower

dimensional affine space (including possibly a single point) that does not intersect the origin. When  $d = 2$  this means that each relative velocity lies in a rational direction. If all relative velocities are parallel, they may be perturbed parallel to this direction while remaining in the horizon, thus there is an  $(N - 1)$ -dimensional horizon (there are two constraints due to energy and parallel momentum conservation, and one extra dimension from the flow direction). The billiard itself is of dimension  $2N - 2$  (two components of momentum conservation), thus we expect a free flight function decaying as  $t^{-(N-1)}$ , which is quite observable in  $N = 3$ , leading to normal diffusion but anomalous Burnett coefficients. If relative velocities are not parallel, there is a lower dimensional space of perturbations and hence a lower dimensional horizon. Note that on  $\mathbb{T}^d$ , it is also easy to see that for particles restricted to parallel hyperplanes, the same decay of  $t^{-(N-1)}$  ensues.

Parallel velocity directions are possible only if the particles are sufficiently small, that is,  $2Nr < 1$ . For a given radius we enumerate non-zero lattice vectors of length  $L > (2Nr)^{-1}$  which correspond to horizons (modulo reflection through the origin). The space perpendicular to the horizon has coordinates  $x_i$ ,  $1 \leq i \leq N$  considered modulo  $L^{-1}$ . However there is also a constraint from the momentum conservation, which fixes the centre of mass:  $\sum x_i = 0$ . We define  $x_i$  so that this constraint remains valid in a horizon, i.e. the  $x_i$  do not translate when reaching the boundaries of a fixed  $L^{-1}$  interval; periodicity is taken account of by imposing that the maximum  $x_i - x_j$  is less than  $L^{-1}$ .

Specialising now to  $N = 3$  we construct orthonormal coordinates on the perpendicular space:

$$\begin{pmatrix} x_1 \\ x_2 \\ x_3 \end{pmatrix} = \frac{1}{6} \begin{pmatrix} 2\sqrt{6} & 0 \\ -\sqrt{6} & 3\sqrt{2} \\ -\sqrt{6} & -3\sqrt{2} \end{pmatrix} \begin{pmatrix} \xi_1 \\ \xi_2 \end{pmatrix}.$$

A fixed ordering of the particles  $x_1 > x_2 > x_3 > x_1 - L^{-1}$  then corresponds to the equilateral triangle  $\xi_2 > 0$ ,  $\sqrt{3}\xi_1 - \xi_2 > 0$ ,  $\sqrt{3}\xi_1 + \xi_2 < 2/(L\sqrt{3})$  and similarly for the other orderings. The effect of finite radius is to tighten the inequalities further,  $x_1 > x_2 + 2r$  etc., and reduce the size of the triangle. Thus in contrast to the lower dimensional horizons associated with incipient horizons discussed in Ref. [18], this non-principal horizon has a convex perpendicular space, for which the visibility function is trivial. For higher  $N$ , the corresponding perpendicular space is likewise an  $(N - 1)$ -dimensional simplex, though not regular; for  $N = 4$  it is an isosceles tetrahedron.

We can now construct the various quantities appearing in Eq. (17). The latter formula assumed a lattice of unit covolume; the covolume of the  $\xi$ -lattice is  $\sqrt{3}$ , and there is a similar factor from the  $y$ -coordinates. We need to divide the formula in Eq. (17) by the covolume raised to the power  $1 - D_H/d$ , i.e.  $\sqrt{3}$ . The double integral comes to  $(L^{-1} - 6r)^4/12$ , taking into account the finite radius of

the balls. We have  $S_1 = 2\pi$  and  $S_3 = 2\pi^2$ . Thus we find for a single horizon

$$F_H(t) = \frac{L^2(2\pi)(L^{-1} - 6r)^4/12}{t^2(2\pi^2)\sqrt{3}(1 - \mathcal{P})}. \quad (42)$$

The excluded volume is a slightly messy integral, giving (in the relevant region,  $0 \leq r \leq 1/6$ )

$$\mathcal{P} = 4\pi r^2(3 - r^2(8\pi + 3\sqrt{3})). \quad (43)$$

For each primitive lattice vector there are six horizons, corresponding to the permutations of the particles, however we divide by two, since opposite lattice vectors correspond to the same horizon. This leads to

$$F(t) \sim \sum'_{\mathbf{l} \in \mathbb{Z}^2} \frac{L^2(L^{-1} - 6r)^4}{t^2 4\pi \sqrt{3}(1 - \mathcal{P})}, \quad (44)$$

where the sum is over primitive lattice vectors  $\mathbf{l}$  of length  $L$ , for which  $L^{-1} - 6r$  is positive.

Figure 2 shows numerical simulations of  $F(t)$  for various  $r$ , together with predictions from Eq. (44). Note that for  $r = 0.16$  which is very close to  $1/6$ , the coefficient is very small and would require greater times and sample sizes to observe. Also, for  $r > 1/6$  there appear to be  $t^{-3}$  asymptotics, due to one-dimensional horizons, for example if  $r < 1/4$  it is possible to have two particles following the same track with equal velocities and another particle in a parallel track moving in the opposite direction. There may be other contributions, however.

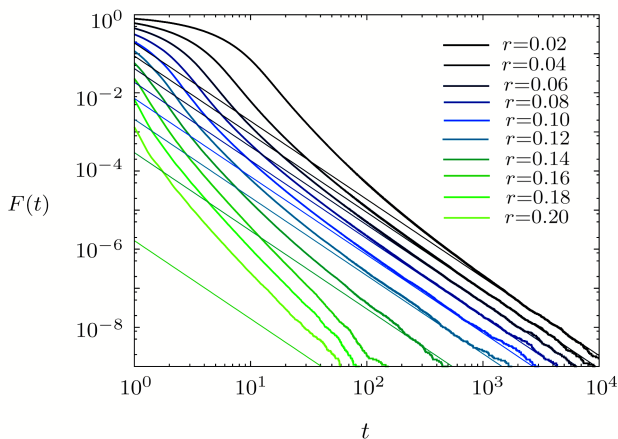


**Fig. 2** Free flight function for three hard disks (thick curves) together with predictions of Eq. (44) for  $r < 1/6$  (thin lines).

For  $r \rightarrow 0$  we can extract the limiting behaviour using Mellin transforms as in Ref. [18]. The result is

$$\lim_{t \rightarrow \infty} t^2 F(t) = \frac{\sqrt{3}}{\pi^2} \left( -\ln r + \gamma + \ln \frac{\pi^{3/2}}{3\Gamma(1/4)^2} - \frac{\zeta'(2)}{\zeta(2)} - \frac{25}{12} \right) + O(r^{3/2-\delta}), \quad (45)$$

where  $\gamma$  is the Euler constant and the correction term assumes the Riemann Hypothesis.

We can conclude the infinite horizon effects are definitely observable in the free flight function, decaying as  $t^{-(N-1)}$  for a configuration in which each particle moves parallel to a single lattice vector. The coefficient decreases with radius, and can be calculated explicitly for  $N = 3$ . These effects are not strong enough to lead to an anomalous diffusion coefficient, but however lead to anomalous Burnett coefficients. The main message, however is that simulations involving a few small particles have spurious long time correlations due to periodic boundary conditions.

## 6.2 Moving Scatterers

Intermediate between the Lorentz gas and many-particle systems lie models with additional degrees of freedom. We have already considered a few such models, the Nosé–Hoover thermostat in Subsec. 3.3(ii) and few-particle systems in Subsec. 6.1. A further class of models retains scatterers with fixed average positions, normally on a periodic lattice, but which are moving in some manner.

**Vibrating** The most obvious effect of a moving boundary is in changing the speed of the particle; the collision law, Eq. (2) generalises to Ref. [128]

$$\mathbf{v}_+ = \mathbf{v}_- - \frac{2\mathbf{n}}{\mathbf{n} \cdot \mathbf{n}} (\mathbf{n} \cdot \mathbf{v}_- - \mathbf{n} \cdot \mathbf{u}), \quad (46)$$

where  $\mathbf{u}$  is the velocity of the boundary. This can lead to unbounded average particle speeds, often termed “Fermi acceleration”.<sup>[129]</sup> References [130–131] discuss this in the context of both stochastic and periodically moving scatterers for the finite horizon Lorentz gas. In particular, the authors of Ref. [130] proposed (the “LRA Conjecture”) that chaotic motion in the corresponding static billiard was sufficient for Fermi acceleration. More recently acceleration has been observed numerically for the ellipse.<sup>[132]</sup> It is also known for a rectangle with a moving barrier<sup>[133]</sup> for which the velocity growth is exponential. Other examples and rigorous results for Fermi acceleration in billiards are reviewed in Ref. [134].

In chaotic billiards the growth of velocity is typically proportional to the square root of the number of collisions, hence linear in time, though slower rates have been observed for “breathing” billiards that retain the same shape.<sup>[128,135]</sup> Boltzmann equations and generalisations have been used to study the distribution of velocities, which typically has an exponential rather than normal tail.<sup>[136]</sup> Recent work in this direction has included periodically oscillating billiards,<sup>[137]</sup> a Lorentz gas with stochastically moving scatterers,<sup>[138–139]</sup> and more general stochastic processes.<sup>[140]</sup>

Infinite horizon effects have recently been considered for vibrating<sup>[141]</sup> and pulsating<sup>[142]</sup> Lorentz models. In this case there is a scenario of “dynamically infinite horizon” in which the billiard has infinite horizon only for part

of the time. Reference [141] showed that horizon effects led to power law correlations between non-interacting particles in a Lorentz channel, while Ref. [142] showed that these effects led to logarithmically enhanced ( $v \sim t \ln t$ ) Fermi acceleration. In view of Subsec. 6.4 below

**Open Problem 9** What rates of acceleration and diffusion are possible for time-dependent polygonal (Ehrenfest) models?

**Rotating** A further generalisation is for each scatterer to have its own degree(s) of freedom. A rotation-inspired model with arbitrarily many degrees of freedom was studied in Ref. [143]. A model with explicit rotating scatterers was proposed and used to study a number of transport phenomena in Refs. [144–145], and a mix of rotating and static scatterers was considered in Ref. [146]. Thermal efficiency properties were studied using many internal degrees of freedom in Ref. [147]. In each of these models, the transfer of energy now permits normal heat conduction, with the dispersing geometry as before used as a source of dynamical randomness.

### 6.3 Flat Points

Another manner in which a Lorentz gas may become non-dispersing is the presence of points of zero curvature. Such a model was considered in the finite horizon case in Ref. [148] where it was shown that two points with local graph  $y = |x|^\beta$  (for  $\beta > 2$ ) forming a period two orbit leads to decay of correlations in discrete time of roughly  $n^{-(\beta+2)/(\beta-2)}$  rather than exponential. Later<sup>[149]</sup> an infinite horizon model was considered, containing an infinite trajectory tangent to a periodic sequence of such flat points, leading to bounds on the free flight function and proofs of nonuniform hyperbolicity.

The following is study of a Lorentz gas with quartic flat points ( $\beta = 4$ ) that has not been previously published. It is similar to Ref. [148] in that the horizon is finite, however the flat points lead to translating periodic orbits, which enhance the rate of diffusion. We will see that the quartic flat point is just sufficient to make the fourth order Burnett coefficient diverge logarithmically, leading to anomalous convergence effects.

The scatterers are ovals defined in local polar coordinates  $(r, \phi)$  by

$$r = \frac{5 - (-1)^{I+J} \cos(2\phi)}{12}, \quad (47)$$

thus having semimajor axis  $1/2$  and semiminor axis  $1/3$ . The centres of the scatterers are located at points of the integer lattice,  $(I, J) \in \mathbb{Z}^2$ . The effect of the sign is to rotate scatterers at odd points by  $\pi/2$ , a configuration with finite horizon and no scatterers touching, see Fig. 3.

The symmetries are those of a square, reflection in both axes and in  $y = x$ , the latter with a spatial translation. Thus the nonzero cumulants up to order four are

$$Q_{20} = Q_{02} = M_{20}, \quad Q_{40} = Q_{04} = M_{40} - 3M_{20}^2, \quad \text{and} \\ Q_{22} = M_{22} - M_{20}^2.$$

Each scatterer has an area  $1 - |S| = 17\pi/96 \approx 0.556324$ , so that the area available to the billiard particle in each unit cell is  $|S|$ . The perimeter is given by the elliptic integral

$$|\partial S| = \frac{\sqrt{5}}{3} \int_{-\infty}^{\infty} \frac{\sqrt{2t^4 + 2t^2 + 1}}{(t^2 + 1)^2} dt \approx 2.72244. \quad (48)$$

Now consider the central scatterer ( $I = J = 0$ ). Near the point  $\phi = 0$  we find

$$x = x_0 - \kappa y^4 + \dots, \quad (49)$$

where  $x_0 = 1/3$  and  $\kappa = 81/8$ . Thus the curvature at this point is zero, and it has a quartic shape, which is generic for analytic zero curvature (“flat”) points. Each flat point can reach exactly two other flat points by a free flight and belongs to exactly one marginally unstable translating orbit (modulo time reversal). These orbits translate either in the horizontal or vertical directions, for example the orbit from  $(1/3, 0)$  reaches the flat point  $(2/3, 1)$  and then reflects to reach  $(1/3, 2)$ . Between each pair of flat points it translates one unit in its overall direction of motion (here the  $y$  direction), taking a time  $\tau = \sqrt{10}/3$ . The angle of incidence is  $\theta_0 = \arctan 3 \approx 72^\circ$ . A horizontal version of this orbit can be seen for several collisions in Fig. 3.

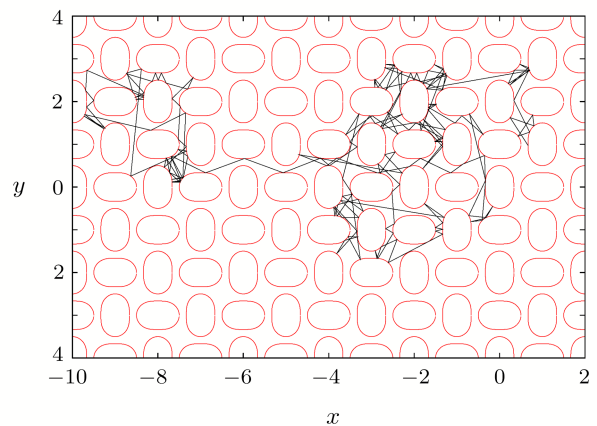


**Fig. 3** A trajectory in the oval Lorentz gas.

Now we perturb the translating orbit. The displacement from the flat point is  $y$  (taken mod 1), while the direction relative to the  $x$ -axis is  $\theta_0 + \theta$  so that both  $y$  and  $\theta$  are small. The approximate collision map is

$$y_{n+1} = y_n + \eta\theta_n, \quad \theta_{n+1} = \theta_n + \psi y_{n+1}^3. \quad (50)$$

For initial conditions  $\theta \approx y^2$  which we will discover are typical, the relative increments of each variable are small, so we can use a continuum approximation

$$\frac{dy}{dn} = \eta\theta, \quad \frac{d\theta}{dn} = \psi y^3. \quad (51)$$

Here,  $\eta = \delta x \sec^2 \theta_0 = 10/3$ , where  $\delta x = 1/3$  is the  $x$  displacement of a single flight, and  $\psi y^3 = -2dx/dy = 8\kappa y^3 = 81y^3$ . Thus we have

$$\frac{d^2 y}{dn^2} = \eta \psi y^3 \Rightarrow \left( \frac{dy}{dn} \right)^2 = \frac{\eta \psi y^4}{2} + A, \quad (52)$$

where  $A$  is a constant of integration, determined from the initial conditions. To reach the translating orbit itself we need  $A = 0$ , which gives separatrix solutions

$$y = \pm \sqrt{\frac{2}{\eta \psi}} n^{-1}, \quad \theta = \mp \sqrt{\frac{2}{\eta^3 \psi}} n^{-2} \quad (53)$$

showing that the scaling  $\theta \approx y^2$  is generally valid approaching the marginal orbit. A second constant is omitted here as it just translates the collision time  $n$ .

For general  $A$  we can combine the first part of Eq. (51) with the second part of Eq. (52) to give an equation for the orbits

$$\eta^2 \theta^2 = \frac{\eta \psi}{2} y^4 + A, \quad (54)$$

which is plotted in Fig. 4. The flow direction is in from the top left and bottom right, and out to the top right and bottom left.

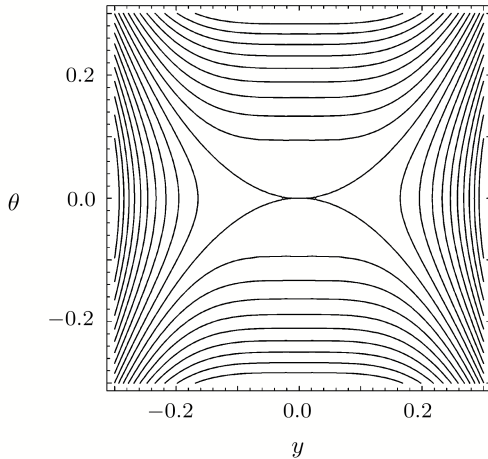


**Fig. 4** Orbits of the flow approximation, moving right at the top and left at the bottom.

Trajectories which remain near the marginal point for a long time have  $A$  close to zero. Let us fix the vicinity of the marginal point as the interval  $y \in [-Y, Y]$  for some arbitrary small constant  $Y$ . The traversal time  $N(A)$  is then the number of iterations needed to move from  $y = -Y$  to  $y = Y$  above the separatrix for  $A > 0$ , or back to  $y = -Y$  to the left of the separatrix for  $A < 0$ . For  $A > 0$  we have

$$\begin{aligned} N(A) &= \int_{-Y}^Y \frac{dn}{dy} dy = \sqrt{\frac{2}{\eta \psi}} \int_{-Y}^Y \frac{dy}{\sqrt{y^4 + 2A/(\eta \psi)}} \\ &= \frac{\Gamma(1/4)^2}{(8\pi^2 \eta \psi A)^{1/4}} + O(Y^{-1}). \end{aligned} \quad (55)$$

For  $A < 0$  we have

$$N(A) = \int_{-\theta(Y)}^{\theta(Y)} \frac{dn}{d\theta} d\theta = (8\eta^3 \psi)^{-1/4} \int_{-\theta(Y)}^{\theta(Y)} \frac{d\theta}{(\theta^2 - A/\eta^2)^{3/4}}$$

$$= \frac{\Gamma(1/4)^2}{(32\pi^2 \eta \psi |A|)^{1/4}} + O(Y^{-1}), \quad (56)$$

where  $\theta(Y) = \sqrt{(\psi Y^4)/(2\eta) + A}$  and both integrals were done with *Mathematica*. Note that the order of the relevant limits is  $A \rightarrow 0$  at fixed  $Y$  giving the long flight behaviour, followed by  $Y \rightarrow 0$ . Thus we can use  $Y = \infty$  in the above integrals. Physically, for very long flights, almost all the collisions are very close to the marginal point, so the size of the considered region becomes irrelevant.

We can now calculate the asymptotic coefficient of the probability of a long flight. We cut a long billiard trajectory into  $M$  segments with displacement  $\mathbf{x}_i$ ,  $i = 1, \dots, M$  and continuous time  $t_i$ . Each segment is either a single collision, or a flight following the marginal orbit for some time, so that correlations are expected to decay exponentially in the number of segments. The continuous time is  $t_i = |\mathbf{x}_i|$  for single collisions and  $t_i \approx \tau |\mathbf{x}_i|$  for very long segments; recall that  $\tau = \sqrt{10}/3$  in the present example. The total displacement and time are thus

$$\Delta = \sum_i \mathbf{x}_i, \quad T = \sum_i t_i \sim \bar{t} M, \quad (57)$$

with an unknown (but ultimately irrelevant) constant  $\bar{t} \approx 1$ .

The anomalous behaviour arises from the long tail in the distribution of  $\mathbf{x}_i$ . Its density function  $p(\mathbf{x})$  is concentrated mostly around the origin, but has tails along the  $x$  and  $y$  axes due to the marginal orbits in these directions. Each long trajectory of at least  $N$  collisions near the marginal orbit enters the region of the marginal orbit  $|y| = Y$  (or corresponding expression involving  $x$ ) exactly once if  $N$  is sufficiently large. From the above calculation, the first collision lies in the region

$$-\frac{C}{N^4} < A < \frac{4C}{N^4}, \quad (58)$$

where  $C = \Gamma(1/4)^8/(32\pi^2 \eta \psi) = \Gamma(1/4)^8/(8640\pi^2) \approx 0.350135$ . This region corresponds to intervals

$$\delta\theta = \frac{5C}{\sqrt{2\eta^3 \psi}} \frac{1}{Y^2 N^4}, \quad \delta y = \sqrt{\frac{\eta \psi}{2}} Y^2, \quad (59)$$

where the first expression is found by combining Eqs. (54) and (58) for small  $A$ , and the second is just an approximation for the change in  $y$  due to a collision at  $|y| = Y$ , following from a combination of Eqs. (50) and (54), again for small  $A$ .

The measure of one of the above regions with respect to the equilibrium measure of the billiard map in the torus is

$$\frac{\cos \theta_0 \delta\theta \delta y}{2|\partial S|} = \frac{\sqrt{10}C}{8\eta|\partial S|N^4}. \quad (60)$$

Thus, the expected number of excursions of more than  $N$  collisions in a trajectory of total length  $T$  is given by

$$\frac{\sqrt{10}CT}{\eta \bar{\tau} |\partial S| N^4} = \frac{\sqrt{10}\Gamma(1/4)^8 T}{300\pi^3(96 - 17\pi)N^4}, \quad (61)$$

where the factor of 8 takes account of the four orbit directions (up, down, left, right) and the two entry points

$y = \pm Y$  (or the same with  $x$ ) of the marginal orbit. The mean free path between collisions is  $\bar{\tau} = \pi|S|/|\partial S|$  as for any 2D billiard table. Strictly speaking this is for the entry to the marginal point; if  $N > T/\bar{\tau}$  (very unlikely), clearly the collisions cannot all take place in the interval. A typical interval will have many excursions, with the largest almost always  $O(T^{1/4})$  according to the above formula.

This gives the tail of the density function  $p(\mathbf{x})$  as

$$\int_Y^\infty dy \int_{-\infty}^\infty dx p(x, y) \sim \frac{D\bar{t}}{Y^4} \quad Y \rightarrow \infty, \quad (62)$$

where

$$D = \frac{\sqrt{10}\Gamma(1/4)^8}{1200\pi^3(96 - 17\pi)} \approx 0.0595772, \quad (63)$$

is an explicit constant. The factor of 4 appears since this is one of four tails,  $T = \bar{t}M$  as above, and the displacement at each collision  $\delta y = 1$  so  $Y = N$ .

The above asymptotic implies that fourth moments of  $p(\mathbf{x})$  diverge. A finite sample will have

$$\frac{1}{M} \sum_i y_i^4 \approx 2 \int_{E_1}^{E_2 M^{1/4}} y^4 \frac{4D\bar{t}}{y^5} dy \sim 2D\bar{t} \ln M, \quad (64)$$

where  $E_1$  and  $E_2$  are constants of order unity, and the  $M^{1/4}$  gives the scale of the largest excursion. The factor of 2 gives the two tails in the  $y$  direction contributing to this moment. The sum of  $x_i^4$  is equivalent, while the mixed even fourth moment  $x^2 y^2$  and second order even moments  $x^2$  and  $y^2$  are small in all tails and yield finite constants. The odd moments cancel by symmetry, and are of size  $M^{-1/2}$ , at least up to fourth order.

Referring back to Subsec. 2.3 we have the Burnett coefficient

$$24B_{1111} = \lim_{T \rightarrow \infty} \frac{Q_{40}}{T}. \quad (65)$$

Here,  $\langle \rangle$  is an ensemble at fixed  $T$ , so that the fourth moment is finite (unlike for fixed  $M$ ). A typical trajectory has  $M \approx T/\bar{t}$ . Expanding the  $\Delta$  terms, assuming the  $x_i$  are independent and have zero odd moments gives

$$\begin{aligned} 24B_{1111}(T, 1) &= \frac{1}{T} \sum_i [\langle x_i^4 \rangle - 3\langle x_i^2 \rangle^2] \\ &= 2D \ln T + O(1). \end{aligned} \quad (66)$$

This is the typical Burnett coefficient found for a single trajectory of length  $T$ . The arguments are the time and the sample size over which it is averaged. This is not however its expected value, which includes the distribution of  $p(x, y)$  up to the maximum length  $T$ . Truncating at the maximum  $T$  rather than the typical  $T^{1/4}$  gives a further factor of 4 for the Burnett coefficient as usually defined, that is, averaged over an arbitrarily large sized sample

$$24B_{1111}(T, \infty) = \frac{\langle \Delta_x^4 \rangle - 3\langle \Delta_x^2 \rangle^2}{T} \sim 8D \ln T. \quad (67)$$

The constant  $8D$  comes to about 0.476 618, so agreeing with the numerically fitted 0.485 in Fig. 5, and exhibiting an anomaly similar to the anomalous convergence of the

second moment observed in the diffusion case 4.2: The logarithmic Burnett coefficient is a factor of four greater than its typical value estimated from a single trajectory of the same length. In other words, while a typical trajectory of fixed continuous time  $T$  has a maximum excursion of order  $T^{1/4}$  in the limit  $T \rightarrow \infty$ , the fourth moment picks up the full support up to  $T$ . The fixed  $M$  moment is likewise infinite, as it picks up contributions from arbitrarily long excursions.

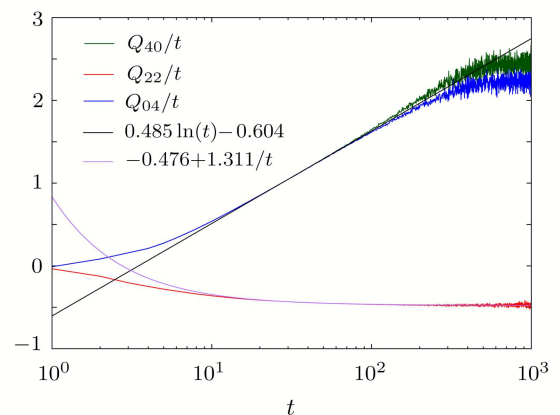


**Fig. 5** Logarithmic divergence of Burnett coefficients, using a trajectory of length  $7.41 \times 10^{10}$  time units split into segments of length  $t$ , and relevant fits.

For a sample size  $T^\alpha$ , there are  $M = T^{\alpha+1}$  excursions, so that the largest is likely to be of order  $(T)^{(\alpha+1)/4}$  leading to an estimate  $2D(\alpha+1) \ln T$  where this is less than  $8D \ln T$ . Some decrease is indeed observed to the right of Fig. 5, but also random fluctuations. More properly, with high probability we expect for a sequence of trajectories of increasing length

$$\lim_{T \rightarrow \infty} \frac{24B_{1111}(T, T^\alpha)}{\ln T} = 2D \max(\alpha+1, 4). \quad (68)$$

Of course, this would require careful arguments and estimates to justify use of the various assumptions, and it may require unreasonably long times in practice before the  $\ln T$  damps the nonleading contributions.

The long flights are only in the coordinate directions, and do not lead to diverging second moments. Thus

$$24B_{1122} = \lim_{T \rightarrow \infty} \frac{Q_{22}}{T} \quad (69)$$

approaches a finite limit as in the figure. It would be interesting to see if the logarithmic Burnett coefficients and anomalous convergence lead to corresponding effects in application areas, from local limit theorems to molecular dynamics.

#### 6.4 Polygonal Scatterers

The  $\beta \rightarrow \infty$  limit of the infinite horizon model with flat points considered in Ref. [149] is that of a square. If there are no points with non-zero curvature, the Lyapunov exponents and entropy are zero, and dynamics is dominated

by the remaining singularities, the corner points. Polygonal billiards thus have properties very different to the dispersing case, and have been under very active investigation recently.

For billiards inside polygons, angles of the form  $\pi/n$  are removable singularities. Thus the polygons with angles  $(\pi/2, \pi/2, \pi/2, \pi/2)$ ,  $(\pi/2, \pi/4, \pi/4)$ ,  $(\pi/2, \pi/3, \pi/6)$ , and  $(\pi/3, \pi/3, \pi/3)$  are completely regular, as are polyhedra associated with Coxeter groups.<sup>[150]</sup> Other polygons with angles a rational multiple of  $\pi$  can be mapped to translation surfaces of finite genus, and any trajectory can have only a finite number of velocity directions. These have been widely studied for the last decade, with many results surveyed in Ref. [11]. The flow is uniquely ergodic in almost all directions,<sup>[151]</sup> weak mixing in almost all directions for most regular polygons,<sup>[152–153]</sup> and rational polygonal billiards are never strong mixing.<sup>[154]</sup> Irrational angles are much more difficult to study. In some cases there is numerical evidence of strong mixing,<sup>[155]</sup> which is widely disbelieved but not disproved, while in others, non-ergodicity.<sup>[156]</sup> A well known problem is Ref. [157].

**Open Problem 10** Do all triangular billiards have at least one periodic orbit?

An extended billiard with square scatterers is called the Ehrenfest wind-tree model, proposed in 1912 by and Ehrenfest.<sup>[158]</sup> The original model, like the original Lorentz model, had dilute randomly placed scatterers (“trees”), which were parallel, for example with their diagonals along the axes. The particle (“wind”) in the original model had an angle of incidence of  $\pi/4$  at each collision, moving always parallel to the  $x$  or  $y$  axis. The corresponding three-dimensional model (with parallel rhombic dodecahedra) seems never to have been studied, however the other conditions have been relaxed, allowing other particle directions, non-parallel orientations, and other polygonal scatterers. As with the Lorentz gas, we first consider periodic configurations.

The first rigorous study of the periodic wind-tree was Ref. [159], describing orbits with angle of incidence  $\pi/4$  as above, for which the dynamics reduces to that of a rotation. For rectangular scatterers of size  $((1 + \alpha)/4, (1 - \alpha)/4)$ , rational  $\alpha$  leads to orbits periodic in then reduced space (hence periodic or translating in the full space). For irrational  $\alpha$  information about the orbit can be obtained using the arithmetic properties (specifically the continued fraction expansion) of  $\alpha$  to obtain a logarithmically diverging sequence of points on the trajectory, hence showing that it is unbounded.<sup>[159]</sup>

More general directions and models require the study of more general interval exchange transformations than rotations, so that the next major result did not come until Ref. [160]. Here it was shown that for rectangles with rational lengths that (in lowest form) have odd numerator and even denominator, there is a dense set of rational

directions for which the dynamics is periodic, and that for almost all directions the dynamics is recurrent. Also, for rectangles with even numerator and odd denominator, there is a dense set of rational directions for which no trajectory is periodic and almost all directions have a logarithmically diverging sequence of points. Thus for generic parameter values (in a topological sense), the dynamics is recurrent, has a dense set of periodic points, and (at least) logarithmically divergent trajectories for almost all directions.

Despite the recurrence results, almost all wind-tree and similar models are non-ergodic in almost all directions<sup>[161]</sup> (in contrast to the finite and infinite horizon Lorentz gases above). Finally, Ref. [162] gives a detailed calculation using theory for translation surfaces developed in recent years showing that almost all wind-trees and directions have  $\limsup \ln |\Delta| / \ln t = 2/3$ ; presumably this is true for typical displacements as well, though it is almost certainly too much to expect a limiting distribution.

Diffusion in a polygonal honeycomb lattice was considered in Ref. [163]. The numerical simulations show  $\langle \Delta^2 \rangle \sim t^{1.72}$  with an anisotropic distribution, due to long flights in six equally spaced directions.<sup>[163]</sup>

A number of authors have performed numerical simulations for polygonal channels, that is, a two-dimensional geometry confined between parallel walls and periodic in the direction parallel to the walls. Variables include whether the horizon is finite, whether scatterers are parallel, whether angles are rational or irrational multiples of  $\pi$ . See for example Refs. [164–166]. The observed diffusion included normal and anomalous with various exponents, but a general theory appears to be absent.

**Open Problem 11** Classify diffusive regimes for polygonal channels.

A deceptively simple example of a Lorentz channel, a “barrier billiard” consists of two parallel walls with periodic infinitely thin spikes protruding perpendicular to one or both walls; models of this type were considered in Refs. [167–168]. For small spikes in one of the walls, this is a retro-reflector, reversing almost all incoming trajectories;<sup>[169]</sup> it is also one of the models shown to be non-ergodic in almost all directions in Ref. [161].

An external field and Gaussian thermostat have also been considered. This leads to transient behaviour followed by stable periodic orbits, for a rhombus wind-tree<sup>[170–171]</sup> and polygonal channels.<sup>[166]</sup> This work including a generalisation to finite particle size, provides insight into anomalous diffusion phenomena in nanopores.<sup>[172–173]</sup> For the polygonal version of the thermostat-type model of Ref. [77] (see Susec. 3.3(ii) above) collapse onto a periodic orbit was observed, but with zero current.

In summary, there are a number of important results for some classes of polygonal scatterers where all bound-

aries are in rational directions, however the case of irrational directions eludes understanding. There are very many difficult remaining open problems.

## 7 Aperiodic Models

### 7.1 Quasiperiodic Models

We now consider aperiodic models, again assuming the dispersing property except where indicated. A quasiperiodic scatterer arrangement is a non-periodic model where the scatterer positions are obtained by the cut-and-project method, that is, taking the intersection of a periodic lattice with an infinite slab (more generally  $\mathbb{R}^d \times S$  with  $S$  a compact set) at some irrational orientation, and projecting transverse to the infinite direction(s) of the slab to obtain a non-periodic set in a lower dimensional space. Note that other and more general definitions are possible, for example using substitutions, tilings or separated nets.<sup>[174]</sup> The transport properties of quasiperiodic Lorentz gases were posed as an open problem in Ref. [127], although quasiperiodic soft potentials had been investigated for some time.<sup>[175–176]</sup>

Using the cut-and-project method, it is possible to reduce the problem to that of a periodic billiard in a higher dimension.<sup>[177]</sup> This permits a natural probability measure for initial conditions, and furthermore allows identification of infinite horizon channels (for relatively small scatterers), which could be analysed as in the periodic case. According to the numerical simulations, diffusion is normal for finite horizon, slightly superdiffusive when there is an infinite horizon, and slightly subdiffusive where the scatterers can overlap.

In the Boltzmann–Grad limit, the free path length is numerically found to be algebraic as in the periodic case,<sup>[178]</sup> and indeed recent methods used to study the periodic Lorentz gas (Subsec. 5.2) can be applied here also,<sup>[179]</sup> also for the union of periodic lattices.<sup>[180]</sup>

### 7.2 Local Perturbations

A periodic Lorentz gas may be locally perturbed, either by changing a finite number of scatterers, imposing a local external field, or imposing a line that the particle reflects from resulting in motion in a half-plane. Reference [181] shows that convergence to Brownian motion with the same diffusion matrix still holds, with differing boundary conditions where appropriate. References [91, 182] made the first steps to extending this to the infinite horizon case by showing analogous behaviour for random walks with unbounded jumps, including with a  $\sqrt{t \ln t}$  scaling.

### 7.3 Decimation and Lorentz Tubes

Recurrence is generic (in a topological sense) for Lorentz and wind-tree (parallel rectangle) models obtained by randomly deleting scatterers subject to a locally finite horizon condition.<sup>[183]</sup> In a similar vein, a Lorentz

tube is a one-dimensional lattice of cells, where the contents of each cell is chosen randomly from a set of dispersing scatterer configurations. Note that the problem of defining the measure for the initial condition of the particle on an infinite space is circumvented: Place the particle in the central cell and choose the scatterer configuration according to the specified distribution. Lorentz tubes in two<sup>[184]</sup> and higher<sup>[185]</sup> dimension with finite horizon are all hyperbolic and almost all are recurrent, ergodic, and K-mixing. The same properties hold in two dimensions when the finite horizon condition is relaxed.<sup>[186]</sup>

For Lorentz gases where the scatterer is randomly changed each time the particle enters a cell, stronger properties (vector almost sure invariance principle) may be shown.<sup>[187]</sup>

### 7.4 Limiting Random Models

Finally, we consider models in which the scatterers are placed randomly without reference to an underlying lattice. Progress has been made mostly for the low density (Boltzmann–Grad) limit so that to a first approximation we may neglect overlapping scatterers and collisions (i.e. collision with the same scatterer more than once in a short time), that is, assume that the scatterer locations are a Poisson process. Lorentz derived a linear Boltzmann equation (linear since the only one particle moves), which was subsequently the subject of more rigorous studies.<sup>[188–189]</sup> In particular, the linear Boltzmann equation holds when the scatterer density converges in probability to its mean (so, not necessarily a Poisson distribution) and any soft potential has finite range.<sup>[189]</sup> The Boltzmann–Grad and other related limits and many particle models were reviewed in Ref. [190], where the above results are restated for  $d \geq 2$ . The Boltzmann equation for the Poisson-distributed two-dimensional Lorentz gas is shown for typical configurations in Ref. [191].

As with the Lorentz tubes, the initial position of the particle may be chosen as the origin, with scatterer positions chosen randomly. This ensemble may be used to define averages and correlation functions as usual. The random Lorentz gas exhibits power law decay of correlations, as  $t^{-d/2-1}$  according to low density kinetic theory. As with similar behaviour for the multi-particle fluids for which it is a prototype, this came as a surprise in the 1960s; these “long time tails” which lead to anomalous and non-analytic behaviour (typically logarithmic terms) in transport coefficients. So, we expect the diffusion coefficient to exist but each Burnett coefficient only in sufficiently high dimension. A detailed history and discussion of these results may be found in Ref. [19].

Kinetic theory methods have more recently been applied to the calculation of other dynamical properties in dilute random Lorentz gases, including the Lyapunov exponents at equilibrium,<sup>[192–195]</sup> with field and thermostat,<sup>[196–197]</sup> and with open boundary conditions.<sup>[198–199]</sup> This approach was also extended to

many particle systems.<sup>[200–201]</sup> Again, logarithmic terms abound.

An applied magnetic field is considered in Refs. [202–204]. The magnetic field bends the trajectories into a circle, making recollisions likely, hence requiring a generalisation of the Boltzmann equation. Adding an additional weak electric field naturally causes a drift with a component perpendicular to the fields, however a scatterer may also cause the particle to be trapped.<sup>[205]</sup> Current and diffusion may be analysed, generalising the case without a magnetic field.<sup>[206]</sup>

Weak coupling limit models, in which the particle is deflected only slightly when it reaches a scatterer, were also reviewed in Ref. [190]. There has been recent progress in showing convergence to the heat equation,<sup>[207]</sup> also with a logarithmic correction.

For the random Ehrenfest model (parallel square scatterers, particle making collision angle  $\pi/4$ ) kinetic theory and numerical simulation show normal diffusion for non-overlapping scatterers but sub-diffusion if the scatterers are allowed to overlap.<sup>[208–210]</sup> Many of the above theorems for the Lorentz gas require only a smooth differential cross-section function and hence apply. However, it is noted in Ref. [211] that an Ehrenfest-like model with parallel crosses and incidence angle of  $\pi/4$  has a finite probability for the particle to immediately return to the previous scatterer, and hence exhibits abnormal behaviour.

### 7.5 Fixed Random Models

The case of randomly placed scatterers of fixed size has also been widely considered theoretically and numerically. For overlapping scatterers at high density there is a percolation transition, at which the diffusion coefficient goes to zero with certain critical exponents and beyond which motion is localised.<sup>[212]</sup> More recent discussion of these phenomena and simulations for the overlapping model in two and three dimensions may be found in Ref. [213].

Random non-overlapping scatterers arise naturally for a mixture of small light particles and large heavy particles in the limit of infinite mass and size ratios. However, this model has resisted rigorous results so far. Even exhibiting the limit of a Poisson distribution of scatterers conditional on them non-overlapping does not appear to have been attempted, although it is the hard potential limit of standard results on the thermodynamic limit of systems with soft potentials; see for example Ref. [214].

In numerical simulations at high density, it can be difficult to find a non-overlapping configuration directly; one approach is to start with a periodic lattice, apply random velocities to all scatterers (as in a full molecular dynamics simulation) and await relaxation to equilibrium. Based on the low density results above, one would again expect normal diffusion but anomalous Burnett coefficients for the random non-overlapping model, and this is what is found. Correlations are found numerically to decay at the

same rate as predicted in the low density limit after a time which increases with the density.<sup>[215]</sup>

Making a diffusive scaling  $L \sim \sqrt{t}$ , numerical simulations of the non-overlapping model exhibit convergence to Brownian motion, for circular and even randomly oriented square scatterers, for which there is no exponential separation of initial conditions.<sup>[216–218]</sup> For the randomly oriented squares in the open case (sufficiently large fixed size and time increasing) it is clear that escape is  $C/t$  (from period three orbits in acute triangles), so there is likely some combination of limits  $t \rightarrow \infty$ ,  $L \sim t^\alpha$  for  $0 \leq \alpha \leq 1/2$  at which there is a transition from anomalous to normal diffusive behaviour.

**Open Problem 12** Does the non-overlapping random Lorentz gas have convergence to Brownian motion?

## 8 Applications

In this final section we summarize the impact that the study of the Lorentz gas has on other fields, past, present and future, drawing together threads from the previous sections.

**Probability** As discussed in Subsec. 4.2, the infinite horizon Lorentz gas, has been a prime example of non-standard convergence to the normal distribution, that is, with logarithmic scaling in time. It is the venue in which the anomalous convergence of moments was discovered, and is currently under investigation. Models with weaker correlations, namely flat points, Subsec. 6.3 exhibit anomalous Burnett coefficients, which are relevant more generally to rate of convergence in local limit theorems.

**Dynamical Systems** The Boltzmann-Sinai ergodic hypothesis<sup>[117]</sup> provided much of the original impetus for ergodic theory, and has only recently been resolved in its original form, Subsec. 6.1. Dispersing Lorentz gases, particularly in higher dimensions, provide a continuing challenge to the study of hyperbolic dynamics with singularities,<sup>[28]</sup> while polygonal models have spurred and made accessible the recently active field of flows on flat surfaces with singularities, Subsec. 6.4. Surfaces of infinite genus, corresponding to billiards with irrational angles, remain a major challenge.

**Statistical Physics** The Lorentz gas has provided a useful model of transport, both diffusion and heat conduction, in that a single moving particle exhibits many features of the full (multi-particle) problem. It was possible to prove validity of the relevant (linear) Boltzmann equation, Subsec. 7.4, as well as providing a simpler context to investigate logarithmic terms in the low density expansion of the diffusion coefficient.<sup>[219]</sup> More recently it has elucidated many of the connections between microscopic dynamics (for example reversibility, Lyapunov exponents, dimensions) and macroscopic transport (for example irreversibility, transport coefficients). See Subsecs 3.3 and 5.1 and also Refs. [2, 20, 216].

**Molecular Simulation** The periodic Lorentz gas is equivalent to two-particle molecular dynamics with periodic boundary conditions, following centre of mass reduction. It has been used as a test-bed for properties of thermostats, additional terms in the equations of motion that take account of effects of the environment, Subsec. 3.3(i). The periodic boundary conditions, while helpful for studying bulk effects, can lead to substantial modifications of the dynamical properties, particularly at low densities, Subsec. 6.1.

**Physics of Transport** Finally, the Lorentz gas and similar models have often been used to model transport on small scales. In this context, the use of polygonal channels for studying nanopores was mentioned in Subsec. 6.4. Lorentz channels have been used to understand thermoelectric efficiency.<sup>[220]</sup> Other examples have included con-

finied fluids,<sup>[221–222]</sup> glasses,<sup>[7]</sup> nuclear collisions,<sup>[223]</sup> and zeolites.<sup>[224]</sup>

### Acknowledgments

The author is grateful for the kind hospitality of the Kavli Institute for Theoretical Physics, China, in July 2013, and also BME Budapest in January 2012, where the work presented in Subsec. 6.3 was commenced. He is also grateful for helpful information and discussions with Peter Bálint (in particular for Subsec. 6.3), Giampaolo Cristadoro, Daniel El-Baz, Pierre Gaspard, Eivind Hauge, Rainer Klages, Paul Krapivsky, Jens Marklof, Gary Morriss, David Sanders (in particular for Subsec. 6.1), Andreas Strömbergsson, Domokos Szász, Bálint Tóth, Corinna Ulcigrai and Henk van Beijeren.

### References

- [1] H.A. Lorentz, *The Motion of Electrons in Metallic Bodies*, in KNAW, Proceedings, Amsterdam **7** (1905) pp. 438–453.
- [2] C.P. Dettmann, *The Lorentz Gas: A Paradigm for Nonequilibrium Stationary States*, Encyclopedia of Mathematical Sciences, **101** (2000) 315.
- [3] N. Chernov and D. Dolgopyat, *Hyperbolic Billiards and Statistical Physics*, in *International Congress of Mathematicians*, **2** (2006) pp. 1679–1704.
- [4] R. Klages, *Microscopic Chaos, Fractals and Transport in Nonequilibrium Statistical Mechanics*, World Scientific, Singapore (2007).
- [5] N. Chernov, *The Work of Dmitry Dolgopyat on Physical Models with Moving Particles*, J. Mod. Dyn. **4** (2010) 243.
- [6] H.J. St. Stöckmann, *Quantum Chaos: An Introduction*, Cambridge University Press, Cambridge (2007).
- [7] B. Vacchini and K. Hornberger, Phys. Rep. **478** (2009) 71.
- [8] J.D. Joannopoulos, S.G. Johnson, J.N. Winn, and R.D. Meade, *Photonic Crystals: Molding the Flow of Light*, Princeton University Press, Princeton, NJ (2011).
- [9] N.I. Chernov and R. Markarian, *Chaotic Billiards*, Amer. Math. Soc. Bookstore, Providence (2006).
- [10] S. Tabachnikov, *Geometry and Billiards*, Amer. Math. Soc. Bookstore, Providence (2005).
- [11] E. Gutkin, Chaos **22** (2012) 026116.
- [12] G.P. Morriss and C.P. Dettmann, Chaos **8** (1988) 321.
- [13] M.P. Wojtkowski and C. Liverani, Commun. Math. Phys. **194** (1998) 47.
- [14] J.A. Roberts and G.R.W. Quispel, Phys. Rep. **216** (1992) 63.
- [15] B. Li, J. Wang, L. Wang, and G. Zhang, Chaos **15** (2005) 015121.
- [16] A. Dhar and D. Dhar, Phys. Rev. Lett. **82** (1999) 480.
- [17] L.A. Bunimovich and H. Spohn, Commun. Math. Phys. **176** (1996) 661.
- [18] C.P. Dettmann, J. Stat. Phys. **146** (2012) 181.
- [19] H. van Beijeren, Rev. Mod. Phys. **54** (1982) 195.
- [20] P. Gaspard, *Chaos, Scattering and Statistical Mechanics*, Cambridge University Press, Cambridge (2005).
- [21] C.P. Dettmann, Ergod. Theor. Dyn. Sys. **23** (2003) 481.
- [22] V.V. Petrov, *Sums of Independent Random Variables*, Springer-Verlag, Berlin (1975).
- [23] P. Nandori, D. Szasz, and T. Varju, arXiv:1210.2231 (2012).
- [24] D.P. Sanders, Phys. Rev. E **78** (2008) 060101.
- [25] J.B. Conrey, Notices of the AMS **50** (2003) 341.
- [26] Y.G. Sinai, Russ. Math. Surv. **25** (1970) 137.
- [27] P. Bálint, N. Chernov, D. Szász, and I.P. Tóth, Asterisque **286** (2003) 119.
- [28] P. Bálint and I.P. Tóth, Nonlinearity **25** (2012) 1275.
- [29] P. Bálint, N. Chernov, D. Szász, and I. Tóth, Annales Henri Poincaré **3** (2002) pp. 451–482.
- [30] P. Bálint and I.P. Tóth, Annales Henri Poincaré **8** (2008) pp. 1309–1369.
- [31] P. Bachurin, P. Bálint, and I.P. Tóth, Israel J. Math. **167** (2008) 155.
- [32] L.S. Young, Ann. Math. **147** (1998) 585.
- [33] N. Chernov, J. Stat. Phys. **127** (2007) 21.
- [34] L.N. Stoyanov, Amer. J. Math. **123** (2001) 715.
- [35] V. Baladi and C. Liverani, Commun. Math. Phys. **314** (2012) 689.
- [36] N.I. Chernov and C. Haskell, Ergod. Theor. Dyn. Sys. **16** (1996) 19.
- [37] J.P. Conze, Ergod. Theor. Dyn. Sys. **19** (1999) 1233.
- [38] K. Schmidt, Compt. Rend. Ser. **327** (1998) 837.
- [39] L.A. Bunimovich and Y.G. Sinai, Commun. Math. Phys. **78** (1981) 479.
- [40] D. Szász and T. Varjú, Ergod. Theor. Dyn. Sys. **24** (2004) 257.
- [41] I. Melbourne and M. Nicol, Ann. Prob. **37** (2009) 478.
- [42] P.M. Bleher, J. Stat. Phys. **66** (1992) 315.
- [43] D.J. Evans and G. Morriss, *Statistical Mechanics of Nonequilibrium Liquids*, Cambridge University Press (2008).

- [44] N.I. Chernov and C.P. Dettmann, *Physica A* **279** (2000) 37.
- [45] J. Machta and R. Zwanzig, *Phys. Rev. Lett.* **50** (1983) 1959.
- [46] R. Klages and C. Dellago, *J. Stat. Phys.* **101** (2000) 145.
- [47] T. Gilbert and D.P. Sanders, *Phys. Rev. E* **80** (2009) 041121.
- [48] C. Angstmann and G.P. Morriss, *Phys. Lett. A* **376** (2012) 1819.
- [49] T. Gilbert, H.C. Nguyen, and D.P. Sanders, *J. Phys. A* **44** (2011) 065001.
- [50] P. Cvitanović, P. Gaspard, and T. Schreiber, *Chaos* (1992) **2** 85.
- [51] G.P. Morriss and L. Rondoni, *J. Stat. Phys.* **75** (1994) 553.
- [52] P. Cvitanović, J.P. Eckmann, and P. Gaspard, *Chaos, Solitons & Fractals* **6** (1995) 113.
- [53] M. Pollicott, *J. Stat. Phys.* **62** (1991) 257.
- [54] R. Klages and J.R. Dorfman, *Phys. Rev. Lett.* **74** (1995) 387.
- [55] R. Klages and J.R. Dorfman, *Phys. Rev. E* **59** (1999) 5361.
- [56] G. Knight and R. Klages, *Nonlinearity* **24** (2011) 227.
- [57] G. Knight, O. Georgiou, C.P. Dettmann, and R. Klages, *Chaos* **22** (2012) 023132.
- [58] G. Keller, P.J. Howard, and R. Klages, *Nonlinearity* **21** (2008) 1719.
- [59] T. Harayama, R. Klages, and P. Gaspard, *Phys. Rev. E* **66** (2002) 026211.
- [60] B. Moran and W.G. Hoover, *J. Stat. Phys.* **48** (1987) 709.
- [61] C.P. Dettmann and G.P. Morriss, *Phys. Rev. E* **54** (1996) 2495.
- [62] C.P. Dettmann and G.P. Morriss, *Phys. Rev. E* **53** (1996) R5545.
- [63] C.P. Dettmann, G.P. Morriss, and L. Rondoni, *Phys. Rev. E* **52** (1995) R5746.
- [64] N.I. Chernov, G.L. Eyink, J.L. Lebowitz, and Y.G. Sinai, *Commun. Math. Phys.* **154** (1993) 569.
- [65] L.S. Young, *Ergod. Theor. Dyn. Sys.* **2** (1982) 109.
- [66] F. Bonetto, N. Chernov, A. Korepanov, and J.L. Lebowitz, *J. Stat. Phys.* **146** (2012) 1221.
- [67] F. Bonetto, N. Chernov, A. Korepanov, and J. Lebowitz, *Speed Distribution of  $N$  Particles in the Thermostated Periodic Lorentz Gas with a Field*, arXiv:1210.7720 (2012).
- [68] N.I. Chernov, *Annales Henri Poincaré* **2** (2001) pp. 197-236.
- [69] N. Chernov and D. Dolgopyat, *Annales Henri Poincaré*, **11** (2010) pp. 1117-1169.
- [70] H.K. Zhang, *Commun. Math. Phys.* **306** (2011) 747.
- [71] N. Chernov, H.K. Zhang, and P. Zhang, *J. Stat. Phys.* **153** (2013) 1065.
- [72] O.G. Jepps and L. Rondoni, *J. Phys. A* **43** (2010) 133001.
- [73] K. Rateitschak, R. Klages, and W.G. Hoover, *J. Stat. Phys.* **101** (2000) 61.
- [74] M. Dolowschiák and Z. Kovács, *Phys. Rev. E* **71** (2005) 025202.
- [75] T. Gilbert, *Phys. Rev. E* **73** (2006) 035102.
- [76] W.G. Hoover and B. Moran, *Chaos* **2** (1992) 599.
- [77] G. Benettin and L. Rondoni, *Math. Phys. Electronic J.* **7** (2001) 3.
- [78] C.P. Dettmann and G.P. Morriss, *Phys. Rev. E* **54** (1996) 4782.
- [79] H. Odbadrakh and G.P. Morriss, *Phys. Rev. E* **60** (1999) 4021.
- [80] F. Galton, *Natural Inheritance*, Macmillan (1889).
- [81] N. Chernov and D. Dolgopyat, *J. Amer. Math. Soc.* **22** (2009) 821.
- [82] J. Piasecki and E. Wajnryb, *J. Stat. Phys.* **21** (1979) 549.
- [83] P.L. Krapivsky and S. Redner, *Phys. Rev. E* **56** (1997) 3822.
- [84] N. Chernov, *J. Stat. Phys.* **94** (1999) 513.
- [85] I. Melbourne, *Proc. Lond. Math. Soc.* **98** (2009) 163.
- [86] P. Bálint and I. Melbourne, *Decay of Correlations for Flows with Unbounded Roof Function, Including the Infinite Horizon Planar Periodic Lorentz Gas*, preprint (2010).
- [87] A. Zacherl, T. Geisel, J. Nierwetberg, and G. Radons, *Phys. Lett. A* **114** (1986) 317.
- [88] H. Matsuoka and R. Martin Jr, *J. Stat. Phys.* **88** (1997) 81.
- [89] D. Sász and T. Varjú, *J. Stat. Phys.* **129** (2007) 59.
- [90] D.I. Dolgopyat and N.I. Chernov, *Russ. Math. Surv.* **64** (2009) 651.
- [91] P. Nándori, *J. Stat. Phys.* **142** (2011) 342.
- [92] P. Bálint, N. Chernov, and D. Dolgopyat, *Convergence of Moments for Dispersing Billiards with Cusps*, preprint (2013).
- [93] I. Melbourne and A. Török, *Ergod. Theor. Dyn. Sys.* **32** (2012) 1091.
- [94] P. Bálint and I. Melbourne, *J. Stat. Phys.* **133** (2008) 435.
- [95] P. Bálint and S. Gouëzel, *Commun. Math. Phys.* **263** (2006) 461.
- [96] P. Bálint, N. Chernov, and D. Dolgopyat, *Commun. Math. Phys.* **308** (2011) 479.
- [97] P. Gaspard and G. Nicolis, *Phys. Rev. Lett.* **65** (1990) 1693.
- [98] T. Gilbert, J.R. Dorfman, and P. Gaspard, *Nonlinearity* **14** (2001) 339.
- [99] M. F. Demers, P. Wright, and L.S. Young, *Ergod. Theor. Dyn. Sys.* **32** (2011) 1270.
- [100] J.P. Eckmann and D. Ruelle, *Rev. Mod. Phys.* **57** (1985) 617.
- [101] H. Kantz and P. Grassberger, *Physica D* **17** (1985) 75.
- [102] S. Viscardy and P. Gaspard, *Phys. Rev. E* **68** (2003) 041205.
- [103] M.F. Demers, *Escape rates and physical Measures for the Infinite Horizon Lorentz Gas with Holes*, preprint (2013).
- [104] P. Tupper and X. Yang, *Proc. Roy. Soc. A* **468** (2012) 3864.
- [105] P. Dahlqvist, *Nonlinearity* **10** (1997) 159.
- [106] F.P. Boca and A. Zaharescu, *Commun. Math. Phys.* **269** (2007) 425.
- [107] V.A. Bykovskii and A.V. Ustinov, *Izv. Ran. Ser. Mat.* **73** (2009) 17.
- [108] E. Caglioti and F. Golse, *Compt. Rend. Math.* **346** (2008) 477.

- [109] J. Marklof and A. Strömbergsson, *Nonlinearity* **21** (2008) 1413.
- [110] J. Marklof and A. Strömbergsson, *Ann. Math.* **172** (2010) 1949.
- [111] J. Marklof and A. Strömbergsson, *Ann. Math.* **174** (2011) 225.
- [112] J. Marklof and A. Strömbergsson, *Geom. Func. Anal.* **21** (2011) 560.
- [113] J. Marklof and B. Tóth, *Superdiffusion in the Periodic Lorentz Gas*, arXiv:1403.6024 (2014).
- [114] J. Marklof, *Invent. Math.* **181** (2010) 179.
- [115] J. Marklof, *The low-density limit of the Lorentz gas: periodic, aperiodic and random*, arXiv:1404.3293 (2014).
- [116] F. Golse, *Recent Results on the Periodic Lorentz Gas, in Nonlinear Partial Differential Equations*, Springer, Barcelona (2012) pp. 39-99.
- [117] D. Szász, *Encyclopedia of Mathematical Sciences* **101** (2000) 421.
- [118] N. Simányi, *Ergod. Theor. Dyn. Sys.* **22** (2002) 281.
- [119] Y.G. Sinai and N.I. Chernov, *Russ. Math. Surv.* **42** (1987) 181.
- [120] A. Krámli, N. Simányi, and D. Szasz, *Ann. Math.* **133** (1991) 37.
- [121] A. Krámli, N. Simányi, and D. Szasz, *Commun. Math. Phys.* **144** (1992) 107.
- [122] N. Simányi, *Invent. Math.* **108** (1992) 521.
- [123] N. Simányi, *Invent. Math.* **110** (1992) 151.
- [124] N. Simányi, *Annales Henri Poincaré* **5** (2004) pp. 203-233.
- [125] N. Simányi, *Invent. Math.* **177** (2009) 381.
- [126] N. Simányi, *Nonlinearity* **26** (2013) 1703.
- [127] D. Szász, *Nonlinearity* **21** (2008) 187.
- [128] B. Batistić and M. Robnik, *J. Phys. A* **44** (2011) 365101.
- [129] E. Fermi, *Phys. Rev.* **75**. (1949) 1169.
- [130] A.Y. Loskutov, A.B. Ryabov, and L.G. Akinshin, *J. Exper. Theor. Phys.* **89** (1999) 966.
- [131] A. Loskutov, O. Chichigina, and A. Ryabov, *Internat. J. Bifurc. Chaos* **18** (2008) 2863.
- [132] F. Lenz, F.K. Diakonov, and P. Schmelcher, *Phys. Rev. Lett.* **100** (2008) 014103.
- [133] K. Shah, D. Turaev, and V. Rom-Kedar, *Phys. Rev. E* **81** (2010) 056205.
- [134] V. Gelfreich, V. Rom-Kedar, and D. Turaev, *Chaos* **22** (2012) 033116.
- [135] B. Batistić, *Fermi Acceleration in Chaotic Shape-Preserving Billiards*, arXiv:1311.4972 (2013).
- [136] C. Jarzynski and W.J. Swiatecki, *Nucl. Phys. A* **552** (1993) 1.
- [137] A.K. Karlis, F.K. Diakonov, and V. Constantoudis, *Chaos* **22** (2012) 026120.
- [138] L. DAlessio and P.L. Krapivsky, *Phys. Rev. E* **83** (2011) 011107.
- [139] G. Gradenigo, A. Puglisi, A. Sarracino, and U.M.B. Marconi, *Phys. Rev. E* **85** (2012) 031112.
- [140] A.V. Kargovsky, E.I. Anashkina, O.A. Chichigina, and A.K. Krasnova, *Phys. Rev. E* **87** (2013) 042133.
- [141] A.K. Karlis, F.K. Diakonov, C. Petri, and P. Schmelcher, *Phys. Rev. Lett.* **109** (2012) 110601.
- [142] C.P. Dettmann and E.D. Leonel, *Europhys. Lett.* **103** (2013) 40003.
- [143] K. Rateitschak, R. Klages, and G. Nicolis, *J. Stat. Phys.* **99** (2000) 1339.
- [144] H. Larralde, F. Leyvraz, and C. Mejia-Monasterio, *J. Stat. Phys.* **113** (2003) 197.
- [145] A. Salazar, F. Leyvraz, and H. Larralde, *Physica A* **388** (2009) 4679.
- [146] J.P. Eckmann and L.S. Young, *Europhys. Lett.* **68** (2004) 790.
- [147] G. Casati, C. Mejía-Monasterio, and T. Prosen, *Phys. Rev. Lett.* **101** (2008) 016601.
- [148] N. Chernov and H.K. Zhang, *Stochastics and Dynamics* **5** (2005) 535.
- [149] H.K. Zhang, *Discr. Contin. Dyn. Sys.* **32** (2012) 4445.
- [150] A.Y. Plakhov and A.M. Stepin, *Russ. Math. Surv.* **53** (1998) 401.
- [151] S. Kerckhoff, H. Masur, and J. Smillie, *Ann. Math.* **124** (1986) 293.
- [152] A. Avila and V. Delecroix, *Weak Mixing Directions in Non-Arithmetic Veech Surfaces*, arXiv:1304.3318 (2013).
- [153] S. Ferenczi, *J. London Math. Soc.* **87** (2013) 766.
- [154] A. Katok, *Israel J. Math.* **35** (1980) 301.
- [155] G. Casati and T. Prosen, *Phys. Rev. Lett.* **83** (1999) 4729.
- [156] J. Wang, G. Casati, and T. Prosen, *Non-Ergodicity and Localization of Invariant Measure for Two Colliding Masses*, arXiv:1309.7617 (2013).
- [157] R.E. Schwartz, *Exper. Math.* **18** (2009) 137.
- [158] P. Ehrenfest and T. Ehrenfest, *The Conceptual Foundations of the Statistical Approach in Mechanics*, Teubner, Leipzig (1912).
- [159] J. Hardy and J. Weber, *J. Math. Phys.* **21** (1980) 1802.
- [160] P. Hubert, S. Lelièvre, and S. Troubetzkoy, *Crelle* **2011** (2011) 223.
- [161] K. Frzcek and C. Ulcigrai, *Invent. Math.* (2013).
- [162] V. Delecroix, P. Hubert, and S. Lelièvre, *Diffusion for the Periodic Wind-Tree Model*, *Ann. Scient. ENS* (to appear) (2014).
- [163] M. Schmiedeberg and H. Stark, *Phys. Rev. E* **73** (2006) 031113.
- [164] D. Alonso, A. Ruiz, and I.de Vega, *Physica D* **187** (2004) 184.
- [165] D.P. Sanders and H. Larralde, *Phys. Rev. E* **73** (2006) 026205.
- [166] O.G. Jepps and L. Rondoni, *J. Phys. A* **39** (2006) 1311.
- [167] R. Zwanzig, *J. Stat. Phys.* **30** (1983) 255.
- [168] J. Hannay and R. McCraw, *J. Phys. A* **23** (1990) 887.
- [169] P. Bachurin, K. Khanin, J. Marklof, and A. Plakhov, *J. Mod. Dynam.* **5** (2011) 33.
- [170] S. Lepri, L. Rondoni, and G. Benettin, *J. Stat. Phys.* **99** (2000) 857.
- [171] C. Bianca and L. Rondoni, *Chaos* **19** (2000) 013121.
- [172] O.G. Jepps, C. Bianca, and L. Rondoni, *Chaos* **18** (2008) 013127.
- [173] C. Bianca, *Commun. Appl. Ind. Math.* **1** (2010) 22.
- [174] Y. Solomon, *Israel J. Math.* **181** (2011) 445.

- [175] E.I. Dinaburg and Y.G. Sinai, *Functional Analysis and Its Applications* **9** (1975) 279.
- [176] G. Zaslavskii, R. Sagdeev, D. Chaikovskii, and A. Chernikov, *Zh. Eksp. Teor. Fiz* **95** (1989) 1723.
- [177] A.S. Kraemer and D.P. Sanders, *Phys. Rev. Lett.* **111** (2013) 125501.
- [178] B. Wennberg, *J. Stat. Phys.* **147** (2012) 981.
- [179] J. Marklof and A. Strömbergsson, *Free Path Lengths in Quasicrystals*, arXiv:1304.2044 (2013).
- [180] J. Marklof and A. Strömbergsson, *Power-Law Distributions for the Free Path Length in Lorentz Gases*, arXiv:1310.0328 (2013).
- [181] D. Dolgopyat, D. Szász, and T. Varjú, *Duke Mathematical Journal* **148** (2009) 459.
- [182] D. Paulin and D. Szász, *J. Stat. Phys.* **141** (2010) 1116.
- [183] S. Troubetzkoy, *J. Stat. Phys.* **141** (2010) 60.
- [184] G. Cristadoro, M. Lenci, and M. Seri, *Chaos* **20** (2010) 023115.
- [185] M. Seri, M. Lenci, M. Degli Esposti, and G. Cristadoro, *J. Stat. Phys.* **144** (2011) 124.
- [186] M. Lenci and S. Troubetzkoy, *Physica D* **240** (2011) 1510.
- [187] M. Stenlund, *Commun. Math. Phys.* **325** (2014) 879.
- [188] G. Gallavotti, *Phys. Rev.* **185** (1969) 308.
- [189] H. Spohn, *Commun. Math. Phys.* **60** (1978) 277.
- [190] H. Spohn, *Rev. Mod. Phys.* **52** (1980) 569.
- [191] C. Boldrighini, L.A. Bunimovich, and Y.G. Sinai, *J. Stat. Phys.* **32** (1983) 477.
- [192] H. van Beijeren and J.R. Dorfman, *Phys. Rev. Lett.* **74** (1995) 4412.
- [193] H. van Beijeren and J.R. Dorfman, *Phys. Rev. Lett.* **76** (1996) 3238.
- [194] A.S. de Wijn and H. van Beijeren, *Phys. Rev. E* **70** (2004) 036209.
- [195] H. Kruis, D. Panja, and H. van Beijeren, *J. Stat. Phys.* **124** (2006) 823.
- [196] H. van Beijeren, J.R. Dorfman, E.G.D. Cohen, H. A. Posch, and C. Dellago, *Phys. Rev. Lett.* **77** (1996) 1974.
- [197] O. Muilken and H. van Beijeren, *Phys. Rev. E* **69** (2004) 046203.
- [198] H. van Beijeren, A. Latz, and J.R. Dorfman, *Phys. Rev. E* **63** (2000) 016312.
- [199] H. van Beijeren and O. Mulken, *Phys. Rev. E* **71** (2005) 036213.
- [200] R. van Zon, H. van Beijeren, and C. Dellago, *Phys. Rev. Lett.* **80** (1998) 2035.
- [201] A.S. de Wijn and H. van Beijeren, *J. Stat. Mech.* **2011** (2011) P08012.
- [202] A.V. Bobylev, F.A. Maa $\phi$ , A. Hansen, and E.H. Hauge, *J. Stat. Phys.* **87** (1997) 1205.
- [203] A. Kuzmany and H. Spohn, *Phys. Rev. E* **57** (1998) 5544.
- [204] A.V. Bobylev, A. Hansen, J. Piasecki, and E.H. Hauge, *J. Stat. Phys.* **102** (2001) 1133.
- [205] N. Berglund, A. Hansen, E.H. Hauge, and J. Piasecki, *Phys. Rev. Lett.* **77** (1996) 2149.
- [206] J. Piasecki, A. Hansen, and E.H. Hauge, *J. Phys. A* **30** (1997) 795.
- [207] G. Basile, A. Nota, and M. Pulvirenti, *A Diffusion Limit for a Test Particle in a Random Distribution of Scatterers*, arXiv:1307.2157 (2013).
- [208] E.H. Hauge and E.G.D. Cohen, *J. Math. Phys.* **10** (1969) 397.
- [209] W. Wood and F. Lado, *J. Comp. Phys.* **7** (1971) 528.
- [210] H. van Beyeren and E.H. Hauge, *Phys. Lett. A* **39** (1972) 397.
- [211] E.H. Hauge, *What can One Learn from Lorentz Models? in Transport Phenomena*, Springer, Heidelberg (1974) pp. 337-367.
- [212] J. Machta and S.M. Moore, *Phys. Rev. A* **32** (1985) 3164.
- [213] F. Höfling and T. Franosch, *Phys. Rev. Lett.* **98** (2007) 140601.
- [214] J. Uńk, *Compendium of the Foundations of Classical Statistical Physics*, in *Philosophy of Science Archive*, URL:philsci-archire.pitt.edu/2691 (2006).
- [215] B.J. Alder and W.E. Alley, *Physica A* **121** (1983) 523.
- [216] C.P. Dettmann and E.G.D. Cohen, *J. Stat. Phys.* **101** (2000) 775.
- [217] C.P. Dettmann and E.G.D. Cohen, *J. Stat. Phys.* **103** (2001) 589.
- [218] B. Li, L. Wang, and B. Hu, *Phys. Rev. Lett.* **88** (2002) 223901.
- [219] J.M.J. van Leeuwen and A. Weijland, *Physica* **36** (1967) 457.
- [220] G. Benenti and G. Casati, *Phil. Trans. Roy. Soc. A* **369** (2011) 466.
- [221] K. Kim, K. Miyazaki, and S. Saito, *J. Phys: Cond. Mat.* **23** (2011) 234123.
- [222] T.O.E. Skinner, S.K. Schnyder, D.G.A.L. Aarts, J. Horbach, and R.P.A. Dullens, *Phys. Rev. Lett.* **111** (2013) 128301.
- [223] N. Borghini and C. Gombeaud, *J. Phys. G* **38** (2011) 124172.
- [224] D.I. Kopelevich and H.C. Chang, *J. Chem. Phys.* **119** (2003) 4573.